UNIVERSITY OF CALIFORNA
RIVERSIDE

Deciphering Regulation of MicroRNA Expression in Disease Vector, *Aedes aegypti*

A Dissertation submitted in partial satisfaction
of the requirements for the degree of

Doctor of Philosophy

in

Genetics, Genomics and Bioinformatics

by

Emre Aksoy

December 2020

Dissertation Committee:
Dr. Alexander Raikhel, Chairperson
Dr. Fedor Karginov
Dr. Naoki Yamanaka

The Dissertation of Emre Aksoy is approved by:

_____

_____

_____
Committee Chairperson

University of California, Riverside

Acknowledgements

I would like express my sincerest gratitude to my PI Dr. Alexander Raikhel for allowing me the opportunity to complete my doctoral degree in his laboratory. Your guidance and support over the past five years has been instrumental in my successes and has enabled me to excel forward as a growing scientist. I am extremely grateful to the members of my committee, Dr. Fedor Karginov and Dr. Naoki Yamanaka, for their continued support over the advancement of my graduate studies. I would like to thank them for their dedication to serving on both my qualifying and defense exam committees as well as providing me with excellent scientific advice that was vital to the completion of my research project.

I would like to thank the assistance of all the Raikhel Lab members for their aid and assistance over the past five years. I would especially like to thank Ellie Cannel who was a great friend during my time in laboratory and whose contribution was essential to my success. I definitely appreciate the above and beyond approach you have that makes coming into lab an enjoyable experience. A special thanks to Dr. Vladimir Kokoza and Dr. Sourav Roy for lending me their knowledge on mosquito expertise. I also to like to acknowledge Dr. Vlastimil Smykal and Dr. Xiufeng Zhang for their mentorship and assistance in different molecular techniques towards my project. I am absolutely grateful for the time they took away from completing their own research projects to lend me their assistance. I would like to thank the previous graduate students Dr. Jisu Ha and Dr. Lisa Johnson for their great friendship and advice when I first arrived at UCR. They definitely made me feel very welcomed in the laboratory from the first day I arrived. In, addition I

would like to thank our current lab members: Dr. Christi Scott, Dr. Lin Ling, Dr. Yike Ding and Dr. Ya-Zhou He, for their advice and recommendations towards my research project. I would also like to give a big thanks to the Entomology Department and all the members of the administrative office who were phenomenal in dealing with and solving all types of different issues during my time here.

Finally, I would like to thank my all the members of my family who have always been a pillar of support for me. A deep gratefulness to both my Mom and Dad for their endless amount of inspiration and love. Their motivation and belief in my ability to succeed were invaluable. Lastly, I would like to thank Kerem and Erin who have shown me great encouragement and positivity throughout this life experience. I look forward to sharing this accomplishment with all of you.

ABSTRACT OF THE DISSERTATION

Deciphering Regulation of MicroRNA Expression
in Disease Vector, *Aedes aegypti*

by

Emre Aksoy

Doctor of Philosophy, Graduate Program in Genetics, Genomics and Bioinformatics
University of California, Riverside, December 2020
Dr. Alexander Raikhel, Chairperson

MicroRNAs (miRNAs) are small non-coding RNAs that play critical roles in post-transcriptional gene expression regulation in eukaryotic organisms. miRNA function is driven by base-pair binding to a complementary mRNA strand which in turn results in mRNA silencing. Here, we employed a novel co-immunoprecipitation technique (CLIP-seq) to identify miRNA-mRNA interactions during the post-eclosion (PE) and blood meal stages of *Aedes aegypti*, and validated miRNA binding using a dual luciferase assay. Next, we investigated the transcriptional factors that govern miRNA expression regulation. We used a double-stranded RNA (dsRNA) knockdown approach to silence *drosha* to enrich for pri-miRNAs in the total RNA pool. Three pri-miRNAs (*miR-276, miR-2940* and *miR-252*) were identified and their respective promoter regions were selected for transcription factor binding analysis using a luciferase based assay. Only one transcription factor, E75, induced luciferase activity and we further explored E75 as part of the juvenile hormone

(JH) hierarchical network. E75 transcript levels could be induced by topical application of JH, and reduced through the blockage of JH pathway by RNAi targeting of the key receptor Met. Using small-RNA sequencing, we found that iMet and iE75 treatments both had a global negative impact on miRNA expression. These findings established the role of E75 within the JH hierarchical network in miRNA activation during the PE phase. We next examined the functional roles of E75 regulated miRNAs, *miRNA-276*, *miRNA-2940* and *miR-252,* during the gonotrophic cycle. Antagomir treatment with Ant-2940-3p resulted in reduced follicle size and number of eggs laid. We performed computational mRNA-miRNA target predictions to elucidate the mRNA gene(s) affected by *miR-2940* knockdown and confirmed by RT-qPCR that the putative target Clumsy (*AAEL002518)* had elevated gene levels from Ant-2940-3p treated fat body tissues. This mRNA-miRNA interaction was confirmed using an *in vitro* dual luciferase assay in *Drosophila* S2 and in native *Ae. aegypti* Aag2 cell lines. Finally, we performed a phenotypic rescue experiment to demonstrate that the elevated expression of *Clumsy* was responsible for the disruption we noted in egg development upon Ant-2940-3p treatment. Collectively, these results confirm the importance of *miR-2940-3p* in the fat body tissue during the PE developmental phase of the gonotrophic cycle.

Table of Contents

List of Figures

CHAPTER I

CHAPTER II

CHAPTER III

CHAPTER IV

List of Tables

CHAPTER II

CHAPTER III

CHAPTER IV

CHAPTER I

Introduction to mosquito biology and the use of hormonal regulation of miRNAs in developing novel inhibitory reproductive control tools

1.1 Mosquitoes as a disease vector and current control strategies

Vector-borne diseases result in over 1 million deaths per year, and place half the world's population at risk to infection[1] (Figure 1). The two mosquito vectors that are largely responsible for disease transmission are *Anopheles gambie*, which transmits the malaria parasite *Plasmodium falciparum*, and *Aedes aegypti*, which transmits various single strand RNA viruses (dengue, yellow fever, chikungunya and Zika). These vectors are largely distributed across the South and Central Americas, sub-saharan Africa and South East Asia. Consequently, these diseases take a major toll in developing countries, inflicting a large public health and economic burden on already strained communities. However, expansion of *Aedes spps*. and hence the diseases they transmit from subtropical regions of the world into highly populated temperate regions, has been a great concern, including for public health in the USA[2]. In 2016, the US government approved a $1.1billion spending budget to prevent the spread and effects of the Zika virus as cases were reported in both

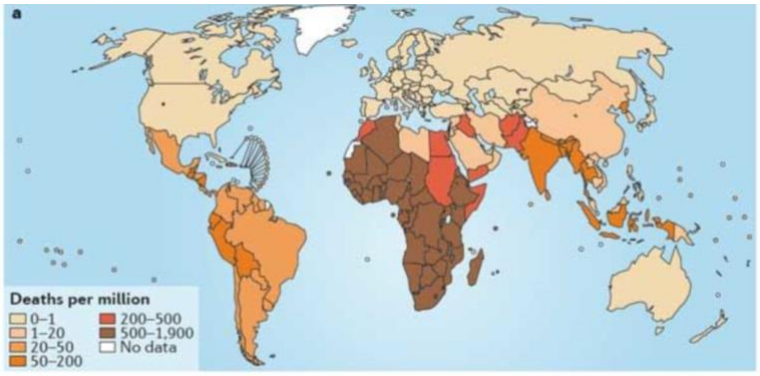

Figure 1.1: Heat map displaying deaths per year on a global stage as a result of vector-borne diseases[1].

Texas and Florida. Methods to prevent these infections are limited, and with the exception of Zika, an efficacious vaccine still does not exist[3].

Multiple approaches beyond insecticide spray have been employed to reduce the burden of disease. These approaches range from environmental modifications (draining wetlands and removing breeding grounds), biological control (using bacterial pathogens or fish that reduce number of mosquito larva in circulating waters) and genetic control (reducing insect fertility to reduce surround populations)[4]. While the combination of all these methods aim to reduce vector populations, two novel applied approaches have recently emerged: releasing either *A. aegypti* colonized with the symbiotic bacterium *Wolbachia* or genetically modified mosquitoes that carry a lethal gene during embryogenesis (Figure 2). *Wolbachia* is a gram-negative bacterium that colonizes the reproductive organs of insects and is estimated to be present in ~20-65% of arthropods world-wide. *Wolbachia* provides female mosquitoes with a reproductive fitness advantage through the process known as Cytoplasmic Incompatibility (CI), ensuring its spread throughout the population[5]. In addition to CI, *Wolbachia* infections in mosquitoes also can enhance vector immunity against viral infections[6]. Currently, capture-release trials in

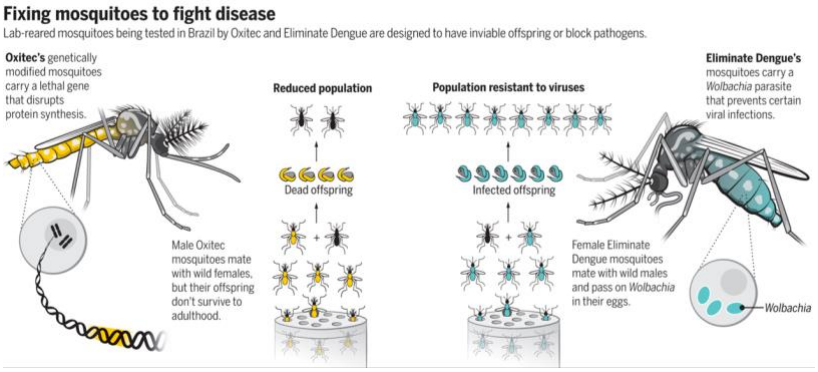

Figure 2.1: Current mosquito approaches to reduce viral disease. (Left) mosquitoes genetically modified to carry a female lethal gene during embryogenesis (designed by Oxitec), (right) mosquitoes injected with *Wolbachia* providing them with a fitness advantage and viral resistance. GRAPHIC: K. SUTLIFF/*SCIENCE*

Brazil and Thailand have shown the ability to reduce the burden of dengue in surrounding communities[7]. Oxitec is a biotech company that has designed a genetically modified mosquito by inserting a tetracycline-repressible transcriptional activator variant (*tTVA*), that blocks protein synthesis during embryogenesis[8]. While previously releases were conducted in Florida to reduce Zika transmission, this program is no longer underway due to community backlash. While release of *Wolbachia* infected virus-resistant mosquitoes is a promising tool, the exact molecular mechanism behind both the reproductive fitness advantage and resistance to viral diseases and their stability over time is poorly understand, and thus a more controllable method is desired.

Reduction of mosquito population density provides a cost-effective method to curb disease. Since *A. aegypti* is also capable of transmitting multiple viruses that circulate in the same geographic region they inhabit, removing or reducing the vector population effectively can inhibit the spread of all viral diseases[9]. During one gonotrophic cycle, one mosquito lays ~100-150 eggs, and is capable of undergoing this reproductive cycle for up to ~3 times during her lifespan. Thus, inhibiting the reproductive cycle can have a significant impact on the immediate and future population densities, and provides a most effective target for biological control efforts. A greater understanding of the underlying molecular mechanism(s) that regulate mosquito reproduction is needed in order to develop a novel inhibitory method.

1.2 Overview of hormonal biology

Hormonal regulation plays a critical role in molecular communication between organs or tissues in all eukaryotic organisms. Normally these processes range from initiating tissue development to regulating metabolism rates, and reproduction; however, these processes are tightly regulated as either over-stimulation or absence of a required signal has been shown to be the root of multiple diseases. For example, 80% of breast-cancer cases are termed “ER-positive”, meaning malignant cells have acquired a mutation causing multiple copies of estrogen receptor to be present on the cell surface. These cells are now over-stimulated by the hormone estrogen, causing cell growth and division. Hormones within the mammalian system composed of diverse structures and molecular components, ranging of peptides (chain of amino acids), steroids (lipid cholesterol molecules) and eicosanoids (fatty acids generally 20C in length). The majority of hormones in the human body are secreted by a gland-like organ to either the same cell (intracrine signaling) or to nearby cells (paracrine signaling) via the circulatory system. Hormones are secreted out into the circulatory system of the organism and initiate their regulatory cascade within their target cell by either binding to a receptor on the cell membrane or by binding an intracellular receptor.

1.3 Identification of the Juvenile Hormone Pathway in Insects

Within insects, hormonal regulation plays a critical role in activating multiple processes, such as reproduction, longevity, differentiation and migratory behavior. Two of the most well studied major classes of insect hormones are Juvenile Hormone (JH), a group

of acyclic sesquiterpenoids, and Ecdysteroids, a group of steroid hormones. Initial interest in studying JH arose from their potential to control insect pests, as chemical analogs of JH (methoprene) were found to have high insecticidal activity and low cross-reactivity in mammals[10]. However, certain insects quickly developed resistance to JH analogs, rending the toxic effect null, and hence research efforts shifted to understanding the molecular mechanism(s) behind JH activation as a means to inactive this cascade[11]. Initial studies sought to identify the receptor responsible for binding JH as a means of developing a novel control method. A P-element mutagenesis screen in *Drosophila melanogaster* for insects that displayed low-levels of toxicity to hormonal treatment led to the identification of the genomic region termed *methoprene-tolerant* (*Met*)[12]. Using inverse PCR from the genomic region surrounding the transposable element led to the identification of the *Met* DNA sequence for complementation experiments. A 5.5-kb transcript was identified using a RNA-probe, and when cloned into transformation vector, rendered Met-insensitive flies to a wild-type phenotype.

Later studies examining the metamorphic phase of the beetle *Tribolium castaneum* would demonstrate the functional importance of Met and JH within insect development. RNAi experiments to target Met inhibited *T. castaneum* developmental and as well as sensitivity to the topical application of JH III and other JH analogs[13]. Subsequently, Met from both *T. castaneum* and *Drosophila* was examined for JH-III binding capacity. Both proteins showed a strong capacity to bind JH III and further examination of the protein domains identified the PAS-B domain as being required of JH III binding[14]. Hence, this

research identified the receptor responsible for JH action and served as a foundational study in understanding the molecular mechanism of JH action in insect species.

1.4 Role of Juvenile Hormone III in adult mosquitoes

In adult female mosquitoes, JH is involved in initiation of tissue maturation process required for vitellogenin production following acquisition of a host blood meal. After pupal emergence, the adult female undergoes a maturation process that is responsible for the development of tissues required for reproduction. The endocrine gland, termed the *corpus allatum*, is responsible for the synthesis and secretion of the critical insect hormone, juvenile hormone III (JH III), into the insect hemolymph[15]. JH hemolymph titers increase over time, reaching peak levels at ~48-50hrs, and decline slowly over the next 5 days[16,17]. One of the critical tissues that undergoes JH III activated maturation is the fat body - the energy storage and utilization center. The fat body stores energy in the form of glycogen and triglycerides, and following a blood meal, synthesizes and secretes lipid and yolk proteins that serve as the nutrient source in the developing oocytes[18]. Interference with the fat body maturation process inhibits the ribosomal biogenesis pathway and results in insufficient production of lipid and yolk leading to an inhibition of egg development[19]. Thus, understanding the transcriptional regulatory network behind JH III mediated activation in fat body is critical to inhibiting the mosquito reproductive cycle.

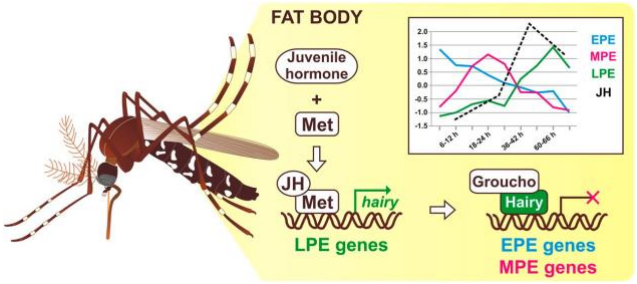

Figure 3.1: Overview of Juvenile hormone (JH) signaling in the mosquito fat body. JH will bind Met, activating the late post-eclosion (LPE), which include Hairy. Subsequently, Hairy will act as a transcriptional repressor and modulate mid post-eclosion (MPE) and early post-eclosion (EPE) gene expression. Image courtesy of Martina Hajduskova (www.biographix.cz)

In the fat body tissue, JH III binds the nuclear receptor *methoprene-tolerant* (Met), a member of the BHLH-PAS transcription factors (TFs), leading to a cascade of events that result in significant changes in both transcriptional activation and repression. JH activation regulates large transcriptional changes within mosquito dynamics, at peak JH III activity ~6,000 genes (30% of the *A. aegpyti* transcriptome) displaying differential expression[20]. This mechanism is mediated through the transcriptional coactivator of the ecdysteroid receptor complex, FISC[21]. Two downstream TFs, Kruppel-homolog 1 (Kr-h1) and Hairy, have been shown to be critical components in the JH III regulatory cascade due to their up-regulation in microarray data that examined early and late post-eclosion (PE) developmental stages and *in vivo* topical application experiment to artificially induce JH activation. Kr-H1 is a C_2H_2 zinc-finger TF implemented in a JH mediated transcriptional response across multiple insects[22]. Specifically in the silkworm, *Bombyx mori*, knockdown of *kr-h1* through double-stranded RNA interference prevents insect metamorphosis during pupal development[23]. In *Aedes*, Met has been shown to directly bind to the promoter region of Kr-h1 through EMSA activity[24], demonstrating its regulatory role over the PE developmental stage. Hairy, a pair-

rule protein, has largely been studied in the context of embryonic segmenting and adult bristle patterning[25]. Hairy will bind to a co-repressor protein, Grouch, and will form a complex that binds to DNA and prevents further transcription of its targets[25]. Through molecular analysis, the co-repressive system mediated by Hairy/Grouch was shown to be evolutionary conserved in the *A. aegypti* fat body tissue[26]. To confirm Met regulatory action of Hairy and Kr-h1, knockdown of *met* was achieved through the use of dsRNA and examined for the expression of downstream targets. The primary ovarian follicle size of dsMet mosquitoes was reduced (~50uM) in comparison to control (~90uM), suggesting that JH maturation and developmental process was inhibited by *met* knockdown. Microarray analysis, and subsequent RNA-seq analysis, from the fat body tissue of *met* knockdown mosquitoes confirmed a reduction in *kr-h1* and *hairy* transcripts[20,26]. Depletion of Met ultimately will lead to an interference of ribosomal biogenesis that has long-lasting effects beyond the PE developmental stage[19]. Interfering with ribosomal biogenesis during this stage prevents the fat body from producing the necessary amount of lipid/yolk levels during vitellogenesis that is required to serve as the nutrient source for egg development, leading to a large reduction in egg numbers.

1.5 Function of the steroid hormone 20-hydroxyecdysone in activating vitellogenesis

Ingestion of a host blood meal triggers a cascade of events that ultimately leads to the activation of vitellogenesis by the fat body tissue. The two major signaling factors in this cascade are amino acids and the steroid hormone 20-hydroxyecdysone (20E). The amino acids will be produced through the digestion of the blood meal in the midgut. 20E production is largely completed by the female ovaries. After the blood meal, Insulin Producing Cells (IPCs) in brain will secrete insulin-like peptide 3 into the hemolymph which will bind to the insulin receptor on the female ovaries to initiate 20E production[27,28]. This mechanism slightly differs between *A. aegypti* and *A. gambie*, where in *A. gambie* the male will produce and transfer 20E to females during mating[29]. The ovaries will secrete 20E into the hemolymph which will bind an intracellular heterodimer receptor composed of two proteins, the Ecdysone receptor (EcR) and ultraspriacle[30] in the fat body cells. This will activate EcR and induce early response genes (E74, E75 and Broad) that eventually lead to vitellogenesis activation[31] (Figure 4). Each factor has multiple isoforms present during the vitellogenic period that regulate different stages of lipid production. For example, E75 has three identified isoforms (termed A, B and C), and through dsRNA targeting each unique isoform has deciphered

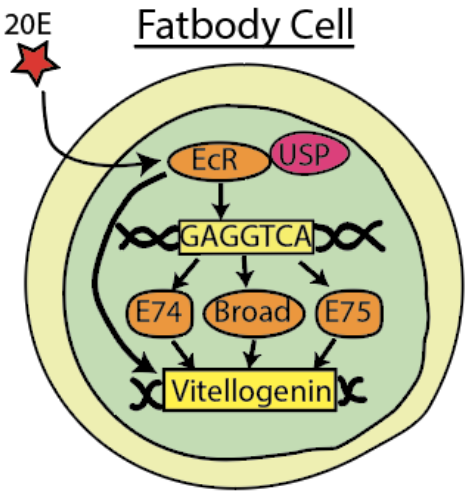

Figure 4.1: Overview of Ecdysone activation in fat body tissue during the blood meal phase. 20E will bind and active the Ecdysone Receptor (EcR) which will bind DNA and upregulate Ecdysone inducible proteins (E74, Broad, E75). Collectively, all factors will bind to vitellogenin promoter for VG activation.

their respective role[32]. Isoform A has been implicated in lipid production at 24hr PBM, while isoform B has no role in lipid production and isoform C is responsible for down-regulating lipid product at 36hr PBM. Collectively, all the factors described above work concurrently and are required to active vitellogenin production. During the PE stage, a GATA (AaGATAr) factor will act as a repressor of yolk producing genes to prevent incorrect transcription of vitellogenesis[33,34]. Once amino acids have entered the fat body tissue through the *slimfast* receptor and activated the target of rapamycin (TOR) pathway[35], a new GATA factor (AaGATAa) will replace the repressor and aid in vitellogenesis activation[36]. Collectively, both 20E and amino acids are required for successful activation of vitellogenesis.

1.6 MiRNAs and their role of in gene expression

MicroRNAs are a class of small non-coding RNAs (containing 20-23 nucleotides in length) that play a critical role in gene silencing in eukaryotic organisms. Since their discovery in 1993 in *C. elegans*[37], their involvement in model eukaryotic organisms as key regulators of developmental processes, cellular function and dysregulation in disease have been explored. MiRNA biogenesis is initiated by RNA polymerase II, which transcribe a pri-miRNA (~400nts) sequence from the genome[38]. The pri-miRNA sequence is then cleaved by the nuclear RNAase III Drosha/DGCRs complex into a pre-miRNA sequence (~70nts) that moves from the nucleus to the cytoplasm through the dsRNA nuclear export protein, Exportin 5[39,40]. Once in the cytoplasm, the RNAse III enzyme Dicer will cleave the pre-miRNA sequence into a double-stranded RNA duplex (~23nt) that contains a two

basepair overhang on the 3' end[41]. The RNA-induced silencing complex (RISC) will incorporate one strand of the duplex and target a region on the mRNA strand for degradation by Argonaute (Ago)[42]. MiRNA regulation is accomplished through the direct binding of the miRNA to the 3' untranslated region (UTR) of a messenger RNA strand. Identifying miRNA targets on the mRNA strand can be challenging due to their non-perfect binding that exists between the two components. Typically a "seed" site exists where the first 2-7 nucleotides of the miRNA will be a perfect match, followed by incomplete base pairing for the additional nucleotides[43]. Bioinformatics programs can take advantage of this knowledge to predict miRNA binding sites through base-pairing interactions, thermodynamics and evolutionary conservation between different species[44-47]. More current techniques have coupled co-immunoprecipitation of Ago coupled with illumina next generation sequence to isolate the mRNA currently bound by Ago (CLIP-Seq)[48].

1.7 MiRNA mediated Hormonal Regulation in *Drosophila*

Early studies deciphering miRNA-mRNA interactions in insects used *Drosophila* as a model organism, due to the availability of tools for genetic manipulation, to understand defects during larval and pupal developmental stages. Developmental stages in *Drosophila* can be linked to changes in circulating hormonal levels, and thus, these studies involved identifying key regulatory factors that were implicated in hormonal regulation. Through transposon-mediated mutagenesis experiments, miRNAs were deleted from the host genome and flies were screened for phenotypic growth defects. Insulin is a critical peptide hormone that reflects nutritional status by regulating circulating sugar levels and fat

metabolism in metazoan organisms and can contribute to overall energy levels[49]. Multiple experiments have indicated that miRNAs contribute to regulating proper insulin signaling during different developmental stages. Through mutagenesis assays, *miR-278* mutants were shown to display a "lean" phenotype, leading to lower triglycerides storage levels in their fat body tissue[50]. Subsequently, these mutants were shown to have higher level of gene expression for multiple insulin-like peptides (small peptides that are secreted by the *corpus allatum* that will bind the insulin-receptor leading to down-stream response), suggestive that the insulin signaling pathway was deregulated in their state. IPCs are located within the brain tissue and are responsible for secreting insulin-like peptides into the hemolymph[51]. Inhibiting the function of IPCs had higher levels of glucose in the hemolymph, similar to a diabetic phenotype, and rendered flies developmentally and metabolically defective[52]. Ilps will bind to the insulin receptor of different tissues and activate a downstream cascade that regulates sugar and lipid metabolism. *MiR-14* and *miR-11* mutants displayed defects in pupal growth and size that were tied to a disruption in the Insulin Signaling Pathway, targeting *sugarbabe* and *Ras85D,* respectively, within IPCs[53,54]. Downstream tissue activation by insulin signaling can regulate a multitude of responses that are mediated by miRNA regulation. For example, *miR-8* mutants displayed small body sizes in the adult stage that was derived by a deregulation specifically in the fat body tissue (Figure 5)[55]. *MiR-8* reduction lead to

Figure 5.1: *MiR-8* mutants display smaller body size. Males (left panel) and Females (right panel) display growth defects in the absence of *miR-8* during developmental stages[53].

evaluated expression levels of *u-shaped* (USH), inhibiting PI3K activity and hence, negatively regulating the insulin response pathway. Ecdysone is steroid hormone critical in regulating tissue development. *MiR-14* mutants showed multiple defects in adult life span, survival rates, increased apoptosis and stress responses, and abnormal fat metabolism; all of which have been linked to increased activity of EcR. *MiR-14* flies had increased gene expression levels of EcR, and reducing EcR through RNAi relieved the abnormal phenotype in mutant[56]. To confirm the interaction between *miR-14* and EcR, a dual luciferase assay was completed to confirm *miR-14* targeting the 3'UTR of the EcR. Overall, these studies collectively demonstrate the involvement of miRNAs in hormonal regulation in *Drosophila* development.

In this dissertation, we aim to explore miRNA regulation and function within the fat body tissue during the post-eclosion developmental phase in *Ae. aegpyt.*. Our research goals are to identify and evaluate miRNAs governed by juvenile hormone activation that lead to proper cellular development production during the gonotrophic cycle. Specifically, we demonstrate a novel reproductive control method by targeting transcriptional factors regulating miRNA expression as a way to block egg development. We highlight a novel role for the transcription factor E75 within the JH hierarchical network as an activator of miRNA expression during this period. Finally, we connect how E75 mediated miRNAs, with a focus on *miR-2940,* activate cellular development and promote the fat body maturation process that in turn leads to successful egg development.

1.8 References

1 Organization, W. H. A global brief on vector-borne diseases. (2014).

2 Armstrong, P. M., Andreadis, T. G., Shepard, J. J. & Thomas, M. C. Northern range expansion of the Asian tiger mosquito (Aedes albopictus): Analysis of mosquito data from Connecticut, USA. *PLoS Negl Trop Dis* **11**, e0005623, doi:10.1371/journal.pntd.0005623 (2017).

3 Dowd, K. A. *et al.* Rapid development of a DNA vaccine for Zika virus. *Science* **354**, 237-240, doi:10.1126/science.aai9137 (2016).

4 McGraw, E. A. & O'Neill, S. L. Beyond insecticides: new thinking on an ancient problem. *Nat Rev Microbiol* **11**, 181-193, doi:10.1038/nrmicro2968 (2013).

5 Werren, J. H. Biology of Wolbachia. *Annu Rev Entomol* **42**, 587-609, doi:10.1146/annurev.ento.42.1.587 (1997).

6 Walker, T. *et al.* The wMel Wolbachia strain blocks dengue and invades caged Aedes aegypti populations. *Nature* **476**, 450-453, doi:10.1038/nature10355 (2011).

7 Dutra, H. L. *et al.* From lab to field: the influence of urban landscapes on the invasive potential of Wolbachia in Brazilian Aedes aegypti mosquitoes. *PLoS Negl Trop Dis* **9**, e0003689, doi:10.1371/journal.pntd.0003689 (2015).

8 Fu, G. *et al.* Female-specific flightless phenotype for mosquito control. *Proc Natl Acad Sci U S A* **107**, 4550-4554, doi:10.1073/pnas.1000251107 (2010).

9 Baly, A. *et al.* Cost effectiveness of Aedes aegypti control programmes: participatory versus vertical. *Trans R Soc Trop Med Hyg* **101**, 578-586, doi:10.1016/j.trstmh.2007.01.002 (2007).

10 Wilson, T. G. The molecular site of action of juvenile hormone and juvenile hormone insecticides during metamorphosis: how these compounds kill insects. *J Insect Physiol* **50**, 111-121, doi:10.1016/j.jinsphys.2003.12.004 (2004).

11 Cerf, D. C. & Georghiou, G. P. Evidence of cross-resistance to a juvenile hormone analogue in some insecticide-resistant houseflies. *Nature* **239**, 401-402 (1972).

12 Ashok, M., Turner, C. & Wilson, T. G. Insect juvenile hormone resistance gene homology with the bHLH-PAS family of transcriptional regulators. *Proc Natl Acad Sci U S A* **95**, 2761-2766 (1998).

13 Konopova, B. & Jindra, M. Juvenile hormone resistance gene Methoprene-tolerant controls entry into metamorphosis in the beetle Tribolium castaneum. *Proc Natl Acad Sci U S A* **104**, 10488-10493, doi:10.1073/pnas.0703719104 (2007).

14 Charles, J. P. *et al.* Ligand-binding properties of a juvenile hormone receptor, Methoprene-tolerant. *Proc Natl Acad Sci U S A* **108**, 21128-21133, doi:10.1073/pnas.1116123109 (2011).

15 Judy, K. J. *et al.* Isolation, Structure, and Absolute Configuration of a New Natural Insect Juvenile Hormone from Manduca sexta. *Proc Natl Acad Sci U S A* **70**, 1509-1513 (1973).

16 Hernandez-Martinez, S., Rivera-Perez, C., Nouzova, M. & Noriega, F. G. Coordinated changes in JH biosynthesis and JH hemolymph titers in Aedes aegypti mosquitoes. *J Insect Physiol* **72**, 22-27, doi:10.1016/j.jinsphys.2014.11.003 (2015).

17 Nouzova, M. *et al.* JH biosynthesis and hemolymph titers in adult male Aedes aegypti mosquitoes. *Insect Biochem Mol Biol*, doi:10.1016/j.ibmb.2018.02.005 (2018).

18 Arrese, E. L. & Soulages, J. L. Insect fat body: energy, metabolism, and regulation. *Annu Rev Entomol* **55**, 207-225, doi:10.1146/annurev-ento-112408-085356 (2010).

19 Wang, J. L., Saha, T. T., Zhang, Y., Zhang, C. & Raikhel, A. S. Juvenile hormone and its receptor methoprene-tolerant promote ribosomal biogenesis and vitellogenesis in the Aedes aegypti mosquito. *J Biol Chem* **292**, 10306-10315, doi:10.1074/jbc.M116.761387 (2017).

20 Zou, Z. *et al.* Juvenile hormone and its receptor, methoprene-tolerant, control the dynamics of mosquito gene expression. *Proc Natl Acad Sci U S A* **110**, E2173-2181, doi:10.1073/pnas.1305293110 (2013).

21 Li, M., Mead, E. A. & Zhu, J. Heterodimer of two bHLH-PAS proteins mediates juvenile hormone-induced gene expression. *Proc Natl Acad Sci U S A* **108**, 638-643, doi:10.1073/pnas.1013914108 (2011).

22 Zhu, J., Busche, J. M. & Zhang, X. Identification of juvenile hormone target genes in the adult female mosquitoes. *Insect Biochem Mol Biol* **40**, 23-29, doi:10.1016/j.ibmb.2009.12.004 (2010).

23 Kayukawa, T. *et al.* Transcriptional regulation of juvenile hormone-mediated induction of Kruppel homolog 1, a repressor of insect metamorphosis. *Proc Natl Acad Sci U S A* **109**, 11729-11734, doi:10.1073/pnas.1204951109 (2012).

24 Cui, Y., Sui, Y., Xu, J., Zhu, F. & Palli, S. R. Juvenile hormone regulates Aedes aegypti Kruppel homolog 1 through a conserved E box motif. *Insect Biochem Mol Biol* **52**, 23-32, doi:10.1016/j.ibmb.2014.05.009 (2014).

25 Fisher, A. L., Ohsako, S. & Caudy, M. The WRPW motif of the hairy-related basic helix-loop-helix repressor proteins acts as a 4-amino-acid transcription repression and protein-protein interaction domain. *Mol Cell Biol* **16**, 2670-2677 (1996).

26 Saha, T. T. *et al.* Hairy and Groucho mediate the action of juvenile hormone receptor Methoprene-tolerant in gene repression. *Proc Natl Acad Sci U S A* **113**, E735-743, doi:10.1073/pnas.1523838113 (2016).

27 Riehle, M. A. & Brown, M. R. Insulin stimulates ecdysteroid production through a conserved signaling cascade in the mosquito Aedes aegypti. *Insect Biochem Mol Biol* **29**, 855-860 (1999).

28 Brown, M. R. *et al.* An insulin-like peptide regulates egg maturation and metabolism in the mosquito Aedes aegypti. *Proc Natl Acad Sci U S A* **105**, 5716-5721, doi:10.1073/pnas.0800478105 (2008).

29 Gabrieli, P. *et al.* Sexual transfer of the steroid hormone 20E induces the postmating switch in Anopheles gambiae. *Proc Natl Acad Sci U S A* **111**, 16353-16358, doi:10.1073/pnas.1410488111 (2014).

30 Martin, D., Wang, S. F. & Raikhel, A. S. The vitellogenin gene of the mosquito Aedes aegypti is a direct target of ecdysteroid receptor. *Mol Cell Endocrinol* **173**, 75-86 (2001).

31 Zhu, J., Chen, L. & Raikhel, A. S. Distinct roles of Broad isoforms in regulation of the 20-hydroxyecdysone effector gene, Vitellogenin, in the mosquito Aedes aegypti. *Mol Cell Endocrinol* **267**, 97-105, doi:10.1016/j.mce.2007.01.006 (2007).

32 Cruz, J., Mane-Padros, D., Zou, Z. & Raikhel, A. S. Distinct roles of isoforms of the heme-liganded nuclear receptor E75, an insect ortholog of the vertebrate Rev-erb, in mosquito reproduction. *Mol Cell Endocrinol* **349**, 262-271, doi:10.1016/j.mce.2011.11.006 (2012).

33 Martin, D., Piulachs, M. D. & Raikhel, A. S. A novel GATA factor transcriptionally represses yolk protein precursor genes in the mosquito Aedes aegypti via interaction with the CtBP corepressor. *Mol Cell Biol* **21**, 164-174, doi:10.1128/MCB.21.1.164-174.2001 (2001).

34 Attardo, G. M., Higgs, S., Klingler, K. A., Vanlandingham, D. L. & Raikhel, A. S. RNA interference-mediated knockdown of a GATA factor reveals a link to

anautogeny in the mosquito Aedes aegypti. *Proc Natl Acad Sci U S A* **100**, 13374-13379, doi:10.1073/pnas.2235649100 (2003).

35 Attardo, G. M., Hansen, I. A., Shiao, S. H. & Raikhel, A. S. Identification of two cationic amino acid transporters required for nutritional signaling during mosquito reproduction. *J Exp Biol* **209**, 3071-3078, doi:10.1242/jeb.02349 (2006).

36 Park, J. H., Attardo, G. M., Hansen, I. A. & Raikhel, A. S. GATA factor translation is the final downstream step in the amino acid/target-of-rapamycin-mediated vitellogenin gene expression in the anautogenous mosquito Aedes aegypti. *J Biol Chem* **281**, 11167-11176, doi:10.1074/jbc.M601517200 (2006).

37 Lee, R. C., Feinbaum, R. L. & Ambros, V. The C. elegans heterochronic gene lin-4 encodes small RNAs with antisense complementarity to lin-14. *Cell* **75**, 843-854 (1993).

38 Lee, Y. *et al.* MicroRNA genes are transcribed by RNA polymerase II. *EMBO J* **23**, 4051-4060, doi:10.1038/sj.emboj.7600385 (2004).

39 Yi, R., Qin, Y., Macara, I. G. & Cullen, B. R. Exportin-5 mediates the nuclear export of pre-microRNAs and short hairpin RNAs. *Genes Dev* **17**, 3011-3016, doi:10.1101/gad.1158803 (2003).

40 Lee, Y. *et al.* The nuclear RNase III Drosha initiates microRNA processing. *Nature* **425**, 415-419, doi:10.1038/nature01957 (2003).

41 Hutvagner, G. *et al.* A cellular function for the RNA-interference enzyme Dicer in the maturation of the let-7 small temporal RNA. *Science* **293**, 834-838, doi:10.1126/science.1062961 (2001).

42 Song, J. J., Smith, S. K., Hannon, G. J. & Joshua-Tor, L. Crystal structure of Argonaute and its implications for RISC slicer activity. *Science* **305**, 1434-1437, doi:10.1126/science.1102514 (2004).

43 Lewis, B. P., Burge, C. B. & Bartel, D. P. Conserved seed pairing, often flanked by adenosines, indicates that thousands of human genes are microRNA targets. *Cell* **120**, 15-20, doi:10.1016/j.cell.2004.12.035 (2005).

44 Kruger, J. & Rehmsmeier, M. RNAhybrid: microRNA target prediction easy, fast and flexible. *Nucleic Acids Res* **34**, W451-454, doi:10.1093/nar/gkl243 (2006).

45 Kertesz, M., Iovino, N., Unnerstall, U., Gaul, U. & Segal, E. The role of site accessibility in microRNA target recognition. *Nat Genet* **39**, 1278-1284, doi:10.1038/ng2135 (2007).

46 Betel, D., Koppal, A., Agius, P., Sander, C. & Leslie, C. Comprehensive modeling of microRNA targets predicts functional non-conserved and non-canonical sites. *Genome Biol* **11**, R90, doi:10.1186/gb-2010-11-8-r90 (2010).

47 Grosswendt, S. *et al.* Unambiguous identification of miRNA:target site interactions by different types of ligation reactions. *Mol Cell* **54**, 1042-1054, doi:10.1016/j.molcel.2014.03.049 (2014).

48 Chi, S. W., Zang, J. B., Mele, A. & Darnell, R. B. Argonaute HITS-CLIP decodes microRNA-mRNA interaction maps. *Nature* **460**, 479-486, doi:10.1038/nature08170 (2009).

49 Saltiel, A. R. & Kahn, C. R. Insulin signalling and the regulation of glucose and lipid metabolism. *Nature* **414**, 799-806, doi:10.1038/414799a (2001).

50 Teleman, A. A., Maitra, S. & Cohen, S. M. Drosophila lacking microRNA miR-278 are defective in energy homeostasis. *Genes Dev* **20**, 417-422, doi:10.1101/gad.374406 (2006).

51 Wu, Q. & Brown, M. R. Signaling and function of insulin-like peptides in insects. *Annu Rev Entomol* **51**, 1-24, doi:10.1146/annurev.ento.51.110104.151011 (2006).

52 Rulifson, E. J., Kim, S. K. & Nusse, R. Ablation of insulin-producing neurons in flies: growth and diabetic phenotypes. *Science* **296**, 1118-1120, doi:10.1126/science.1070058 (2002).

53 Li, Y., Li, S., Jin, P., Chen, L. & Ma, F. miR-11 regulates pupal size of Drosophila melanogaster via directly targeting Ras85D. *Am J Physiol Cell Physiol* **312**, C71-C82, doi:10.1152/ajpcell.00190.2016 (2017).

54 Xu, P., Vernooy, S. Y., Guo, M. & Hay, B. A. The Drosophila microRNA Mir-14 suppresses cell death and is required for normal fat metabolism. *Curr Biol* **13**, 790-795 (2003).

55 Jin, H., Kim, V. N. & Hyun, S. Conserved microRNA miR-8 controls body size in response to steroid signaling in Drosophila. *Genes Dev* **26**, 1427-1432, doi:10.1101/gad.192872.112 (2012).

56 Varghese, J. & Cohen, S. M. microRNA miR-14 acts to modulate a positive autoregulatory loop controlling steroid hormone signaling in Drosophila. *Genes Dev* **21**, 2277-2282, doi:10.1101/gad.439807 (2007).

CHAPTER II

Identification of juvenile hormone regulated transcriptional factors responsible for miRNA expression

2.1 Abstract

MicroRNAs (miRNAs) are a class of small non-coding RNAs that play critical roles in post-transcriptional regulation of gene expression in eukaryotic organism. MiRNA function is driven by base-pair binding to a complementary mRNA strand which in turn results in mRNA silencing. Here, we first employed a novel co-immunoprecipitation technique (CLIP-seq) to identify miRNA-mRNA interactions during the post-eclosion (PE) and blood meal stages of the *Aedes aegypti* mosquito and validated miRNA binding using a dual luciferase assay. Next, we aimed to determine the transcriptional factors that govern miRNA expression regulation. This task is challenging due to the lack of pri-miRNA annotations in the *Ae. aegypti* genome. A possible reason for this problem is that during the miRNA biogenesis, the initial pri-miRNA transcript is quickly degraded after cleavage by Drosha into the pre-miRNA duplex. As a result of this degradation, *pri-miRNAs* are typically excluded from traditional RNA-seq experiments and absent in the genome annotation processes. Here, we used a double-stranded RNA (dsRNA) knockdown approach to silence *drosha* to prevent pri-miRNA cleavage in order to enrich for the transcript levels of pri-miRNAs in the total RNA pool. Adult female mosquitoes were injected with dsDrosha and the fat body tissue was collected 72 hours post injection. After confirming *drosha* knockdown by RT-qPCR, RNA samples were sent for RNA-seq analysis for *de novo* pri-miRNA discovery. Reads were aligned to the *Ae. aegypti* genome

and enrichment of transcripts mapping near the pre-miRNA locations were manually scanned for the identification of potential pri-miRNAs. In total, three pri-miRNAs (*miR-276, miR-2940* and *miR-252*) were selected for validation and their respective promoter regions were selected for downstream functional analysis. These putative promoter regions were cloned into a luciferase expression vector and examined for transcriptional activity in the presence of different juvenile hormone induced transcription factors. Only one transcription factor, E75, was capable of inducing luciferase activity from the pri-miRNA promoters, suggesting that this transcription factor is a key activator of miRNA expression.

2.2 Introduction

MiRNAs play a critical role in regulating numerous mosquito physiological processes during the life cycle. Currently, there is no information on the involvement of miRNAs during the PE developmental stage. As noted in the Introduction Chapter, JH III activation results in profound changes in gene induction/reduction, and it is possible that some of these changes are also governed by miRNA mediated processes. A recent study in *D. melanogaster* characterized the role of *miR-276* in circadian rhythms through its regulation of *timeless*[1]. In *Ae. aegypti*, JH III activation of *kr-h1* and *hairy* occurs in a light-dependent circadian rhythm during PE development[2]. Identification of miRNA binding sites on mRNA transcripts is technically challenging, and prior methods involved utilizing multiple bioinformatics programs to generate *in silico* prediction tools. New technological advancements have led to genome wide profiling of RNA-protein interactions using crosslinking immunoprecipitation (CLIP) coupled with high-throughput sequencing on an

Illumina platform[3]. Here, we made use of antibodies against *Ae. aegypti* Ago1 in a CLIP-seq protocol from the mosquito fat body during vitellogenesis to elucidate multiple miRNA targets at a single time point with high confidence.

The majority of prior experiments have focused on miRNA-mRNA interactions in terms of deciphering miRNA biological function in reproduction physiology. Another potential avenue for reproductive control could be targeting the key transcription factors that regulate miRNA expression. Blocking transcriptional activity of miRNA expression could serve as a potential method to disrupt miRNA function and block egg development. Previous research efforts have functionally characterized critical transcription factors that regulate mRNA gene expression during this time period. It is likely that these transcription factors can also have the potential to serve as regulators of miRNA expression at this time. While there is no information on hormonal regulation of miRNAs in *Ae. aegypti*, in the *Drosophila* model it has been demonstrated that *miRNA* expression can be correlated with peaks in both juvenile hormone and ecdysone levels during the developmental profile. Early studies followed these findings in *Drosophila* S2 cell line, and identified the ecdysone-specific transcription factor BR-C to be responsible for mediating the expression of the *pri-miRNA* for *let-7*, *miR-125* and *miR-100*[4]. A more recent study in *Drosophila* examined the role of *miR-34* regulation of the ecdysone pathway in innate immunity[5]. This study found that the BR-C transcription factor bound to the *pri-miR-34* promoter as a repressor of *miR-34* expression. In the absence of *miR-34*, the ecdysone factors E75 and E74 were activated and led to induction of an antimicrobial response to bacterial pathogens.

These two initial studies confirm that hormonally regulated transcriptions factors can influence *miRNA* expression.

Identifying the candidate transcription factors for miRNA expression regulation can be challenging due to the lack of information on the promoter elements located upstream of miRNA start sites, which the transcription factors would typically bind to. Currently, the most up to date version of the *Ae. aegypti* genome has only one pri-miRNA annotation for *miR-276*, leaving over 100 pri-miRNAs absent from the database. This issue arises in large part due to the nature of the miRNA biogenesis. Mature miRNAs originate from an RNA strand, termed pri-miRNA, that will quickly be degraded after cleavage by Drosha in the biogenesis pathway. As a result of this degradation early in the biogenesis process, pri-miRNAs are not detected in a standard RNA-seq application, and as a consequence are missing from the genome annotation data. A methodology to enrich for pri-miRNAs addressing this specific issue has been described using a Drosha-knockout human cell line. A CRISPR-cas9 drosha knockout line was developed using the human T-HEK293 cell line, and demonstrated the accumulation of pri-miRNAs in comparison to the wild-type cell line[6]. Performing RNA-seq analysis from this KO-line resulted in a sufficient number of reads for the precise mapping of pri-miRNAs transcriptional start sites in the genome. Two approaches were then used to confirm these findings from RNA-seq results. First, the identified pri-miRNA start sites correlated positively with ChIP-seq datasets for RNA Pol II, the protein complex responsible for transcribing pri-miRNA. Second, the upstream promoter region was enriched for DNA-binding transcription factor motifs, the proteins responsible for recruiting RNA Pol II to the transcriptional start site. Both of these

findings suggest that the methodology that blocks Drosha function can result in the identification of pri-miRNA start sites. We followed this methodology using dsRNA targeted against the *Ae. aegypti drosha* transcript and followed through with RNA-seq analysis for the identification of novel pri-miRNAs and their potential start sites.

We validated the potential promoter regions by utilizing an *in vitro* luciferase based assay in *Drosophila S2* cells. Luciferase expression from the respective *pri-miRNA* promoter region was evaluated following the addition of different juvenile hormone linked transcriptional factors. From the potential transcription factor screen, we found that only ecdysone induced protein 75 (E75) was capable of inducing luciferase expression. Currently, E75 has not been associated with the juvenile hormone hierarchical network and is thought only to primarily function during the 20E-driven vitellogenic stage. Thus, in this chapter we lay the fundamental ground work for demonstrating the potential of E75 as a key regulator of miRNA expression during the JH-regulated PE developmental stage.

2.3 Material and Methods

In Vitro Validation of CLIP-Seq Targets:

PCR products containing full-length *Ae. aegypti* 3′ UTRs (based on AaegL3.3 annotations) were prepared from genomic DNA (gDNA) or FB-specific cDNA templates. gDNA was extracted from whole-body female adults as previously described. TRIzol-isolated total RNA samples from female FBs at 72 h PE and 24 h PBM were reverse transcribed with SuperScript II (Invitrogen). The 3′ UTRs were amplified with primers containing *BsmB*I or *BbsI* sites and cloned downstream of Renilla luciferase in modified

pRL-TK vectors (Promega) using Golden Gate Assembly (NEB): 4 µL H_2O, 0.75 µL *BsmB*I or *BbsI*, 1 µL Tango Buffer, 1 µL 10 nM DTT, 0.25 µL T7 ligase, 1 µL pRL-TK plasmid, 1 µL 10 nM ATP, and 1 µL PCR product, with 10 cycles of 37°C for 10 min and 20°C for 10 min, followed by Plasmid-Safe DNase treatment (Epicentre Biotechnologies) to remove linear DNAs. For selected UTRs, 7mer miRNA seed complements in the AGO1 binding sites were mutated using a Q5 Site-Directed Mutagenesis kit (NEB).

HEK T-REx-293 cells were cultured in 96-well plates in 10% FBS in DMEM and transfected at 50–70% confluency with Renilla reporter plasmid and pGL3 (firefly luciferase) transfection normalization plasmid at 100ng each, and miRNA mimic or AllStars negative control siRNA (Qiagen) at 100nM using Attractene (Qiagen). Cells were assayed 24 hr posttransfection using the Dual-Luciferase Reporter Assay System (Promega). The effects of miRNA mimics are presented by means of ratios of $(\text{Renilla/Firefly})_{\text{miRNA-mimics}}/(\text{Renilla/Firefly})_{\text{Allstar}}$. Each experiment consisted of three technical replicates and repeated independently three times. Statistical significance of the biological replicates was calculated using unpaired one-tailed Student's *t* tests, because it is generally accepted that miRNAs mostly repress target gene expression through post-transcriptional modulation.

Double-stranded RNAi injections:

DsRNAs for *iLuc*, and *iDrosha* were synthesized using the MEGAscript Kit (Ambion). At 12 hr PE, 0.5µg (.25µl of 2µg/µl) dsRNA was injected into the thorax of

adult female mosquitoes. Mosquitoes were allowed to recover for 3-4 days on both H_20 and sugar water before dissection and fat body tissue collection.

Quantitative Reverse Transcription PCR (RT-qPCR):

Total RNA was prepared using Trizol (Invitrogen) following the manufactures protocol. Total RNA was purified using Zymo RNA cleanup kit (R1018) using the in-column DNase treatment (E1010). Total RNA was quantified using a Nanodrop 2000 and 2.5µg was subjected to cDNA synthesis using the SuperScript III Kit (Invitrogen). Expression data was plotted as $2^{-\Delta Ct}$ whereby the cycle threshold (Ct) for the gene of interest is compared with the Ct of the internal control gene. All expression data are plotted as relative expression to *actin*.

RNA-seq Analysis:

Total RNA was sent to BGI for library preparation and next-generation illumina sequencing. mRNA was isolated by poly-A tail pulldown and used for cDNA synthesis. Library preparation was completed under their protocol. Paired reads were mapped to the *Ae. aegypti* Chromosome (AaegL5.1) using HISAT. Afterwards, reads were separated based on whether or not they matched to the current *Ae. aegypti* transcriptome reference using Bedtools. For reads that mapped to the *Ae. aegypti* transcriptome, transcript abundance (FPKM) was estimated using Stringtie and differential expression analysis was completed using Ballgown. For reads that did not match to *Aedes* transcripts, reads from all samples were concatenated and used for assembly of novel transcripts in Stringtie.

FPKM were estimated for individual samples against the newly generated reference of novel transcripts and differential expression analysis was completed using Ballgown.

Cell culture and dual luciferase assay:

Drosophila S2 cells (Invitrogen) were maintained at 28°C in Schneider's *Drosophila* medium (Gibco, Life Technologies) supplemented with 10% heat-inactivated FBS (Gibco, Life Technologies) and 1x Penicillin-Streptomycin (ThermoFisher Scientific). Candidate promoter regions upstream of target genes were amplified by PCR. An *NehI* cleavage site was placed on the forward primer and a *KpnI* cleavage site was placed on the reverse primer for ligation into the pGL4.17 vector (Promega). pCopia (*renilla*) luciferase vector was used as a control vector for normalization in the transfection experiments. For Met, FISC, Hairy, Groucho and E75 protein expression, CDS regions were cloned into the pAc5.1-V5 vector (Invitrogen), respectively. Transfections were performed using Fugene HD (Promega) following standard protocols (0.5ug of DNA per well, 3.0:1 ratio of transfect reagent:DNA). For Met/FISC transfections, 6 hr post transfection either 1µl of 1µg/µl of JH III or ethanol was applied to the media. S2 cells were collected 24 hr post transfection and used in the Dual Luciferase Reporter Assay System (Promega). Treatments were performed in triplicates and transfection experiments were performed three times independently.

2.4 Results

To access potential miRNA-mRNA interactions, Ago1 CLIP-seq peak binding data was cross-referenced with microarray data from 72 h PE and 24 h PBM. From this comparison, a number of potential candidate miRNA-mRNA interactions were selected for *in vitro* validation using the dual-luciferase cell culture based assay. Experiments were completed in a human cell line (HEK293), rather than the *Drosophila* S2 cell line, to eliminate potential background noise from endogenous miRNAs. In total, 12 candidate 3'UTR were amplified by PCR and cloned into the psiCheck2 luciferase reporter vector, respectively. Cells were transfected either with the cognate miRNA mimic, or with a scrambled control RNA mimic and harvested for luciferase measurements 24 hr post transfection, respectively. Ten of the 12 candidate UTRs analyzed displayed a repression in luciferase expression when transfected with the candidate miRNA in comparison to the scrambled control. To verify the miRNA binding site, we mutated the "seed" complementary region in the candidate UTR and repeated the transfection experiments. Four out the 10 mutated UTRs returned the original levels of luciferase expression, indicating that the candidate miRNA no longer capable of binding to the UTR and confirming the miRNA-miRNA targeted interaction. Specifically, we confirmed the binding of *miR-286b* to a transcript coding an unknown protein (*AAEL010015*), *miR-11* to an unknown protein (*AAEL013070*) and *miR-275* to glutamate semialdehyde dehydrogenase (*AAEL006834*) and GSH/elf-1 transcription factor (*AAEL000577*) (Figure 1). This experiment signifies the importance of miRNA mediated gene expression regulation within the fat body tissue during the *Ae. aegypti* gonotrophic cycle. It also

highlights the potential avenues for blocking the miRNA-mRNA regulation as an approach to disrupt fat body function in egg development. Another possible opportunity of mosquito control could involve blocking the transcription factors regulating miRNA expression as a method to disrupt the miRNA-mRNA interactions. However, information on the promoter region(s) corresponding to the individual pri-miRNAs is required in order to evaluate the probable factors regulating miRNA expression.

We performed RNAi for targeting Drosha (*AAEL008592*) expression from adult female mosquitoes and collected fat body tissue at 72 h PE. We evaluated the knockdown efficiency of our treatment by RT-qPCR and found an ~80% reduction in *drosha* levels relative to that from the iLuc control group (Figure 2A). We subsequently measured gene expression levels of the *pri-miRNA-276* (*AAEL027655*) and found an increased level of expression relative to the iLuc control (Figure 2B). These results confirm that the RNAi treatment was both sufficient in reducing *drosha* levels, and led to an enrichment of the pri-miRNA transcripts. We next preformed RNA-seq analysis on the iDrosha and iLuc samples in an attempt to discover novel pri-*miRNAs*. Three biological replicates were included in treatment and control groups, and each biological sample was sequenced to the depth of ~20 million reads (2x100). Reads were mapped to the *Ae. aegypti* reference genome (L5.1) and expression levels were compared between the iLuc and iDrosha groups, respectively. As expected, *AAEL027655* (fc, +3.8 at 72 hr PE) displayed an upregulation within the iDrosha dataset, matching with the RT-qPCR findings. We manually scanned for reads mapping upstream of *pre-miRNA* genomic locations to identify potential pri-miRNAs. We discovered an enrichment of reads located to the pre-miRNA of both *miR-*

2940 and *miR-252* in the iDrosha samples that were absent in the iLuc samples (Figure 2). Using RT-qPCR, we confirmed the enrichment of both pri-miRNAs and selected these three pri-miRNAs (*miR-276*, *miR-2940* and *miR-252*) for further functional promoter analysis.

To determine potential regulators of pri-miRNAs, we utilized a cell based luciferase assay in *Drosophila* S2 cells. Candidate promoter regions were cloned by PCR into the promoter-less firefly luciferase vector (pGL4.17) and transfected with or without protein expression vector (pAc5.1). Initially, we measured luciferase levels from different transcription factors that have previously been characterized during the PE developmental phase, which include Met and FISC (Taiman), Hairy and Groucho or Kruppel-homolog 1, on each of the individual pri-miRNA promoters, respectively (Figure 3). The over-expression of each transcription factor had no effect on the amount of luciferase produced by any of the three candidate promoters tested. Thus, we reasoned that an additional factor was likely responsible for pri-miRNA regulation. We searched previous fat body-specific RNA-seq data during the PE phase for identify additional transcription factors expressed during this phase. E75 (*AAEL007397*) was found to have an equal RPKM level to that of kr-h1, and thus we speculated it could have a regulatory function during this phase. Expression of the E75-RD isoform in our assay increased the amount of luciferase produced by all three candidate promoters, suggesting that this transcription factor is a key activator of miRNA regulation. We next utilized a progressive deletion strategy in order to identify the specific DNA motif bound by E75 on the promoter region for all three candidate promoters (Figure 4, 5 and 6). The 5' region of the promoter plasmids were

truncated until the luciferase activity was equivalent to the promoter-less pGL4.17 plasmid. We found the respective upstream regions for *miR-276* (570-560), *miR-2940* (165-115) and *miR-252* (325-280) to contain the DNA region responsible for E75 binding. To confirm this result, we performed a site-directed mutagenesis assay on the specific DNA region from the wild-type plasmid and found activity levels equivalent to the empty control vector. Mutating a six-base pair region on the *miR-2940* promoter and 13 base pair region on *miR-252* promoter alleviated E75 activity (Figure 7 and 8). Thus, these *in vitro* experiment demonstrate that E75 is an activator of miRNA regulation, and confirm the specific binding site of E75 regulating *miR-2940 and miR-252* expression. We next set out to examine *in vivo* E75 regulation of miRNA expression in the fat body tissue during the PE developmental phase.

2.5 Discussion

Here we set out to identify potential regulators of miRNA expression during the juvenile hormone regulated post-eclosion (PE) developmental phase of the *Ae. aegypti* reproductive cycle. We identified the *Drosophila* homolog of Drosha in *Ae. aegypti*, and successfully implemented an RNAi strategy to inhibit its functional role in the miRNA biogenesis pathway. We performed RNA-seq on the iDrosha treatment group in an effort to discover *de novo* pri-miRNAs. While we discovered novel pri-miRNAs for both *miR-2940* and *miR-252*, respectively, the majority of pri-miRNAs for very abundant miRNAs showed no enrichment in the iDrosha group. The general notion is that pri-miRNAs are poly-adenylated similar to that of mRNA transcripts, and thus should be enriched during

the poly-A pulldown step in mRNA library preparation. However, it is possible that this is not the case, and thus using a rRNA removal method with total RNA may provide a more comprehensive finding.

To identify potential regulators acting on the candidate pri-miRNA promoters, we utilized a transcription factor screen based on the induction of Luciferase levels. We initially tested our previously characterized transcription factors from the JH regulatory cascade, and found that none had any induction effects on the pri-miRNA promoters. However, this result adheres to our general theoretical understanding of the JH hierarchical regulatory pathway. While Met is the key receptor in activing the JH pathway, its function in gene activation is largely thought to be derived from its action on the downstream transcription factors[2,7]. Hairy and Groucho are mainly thought to act as repressors, and thus it is expected they would have no effect on pri-miRNA activation[8]. Lastly, while Kr-h1 has been demonstrated to have both an activator and repressor function for gene expression in *Ae. aegypti*, our previous experiments have only shown its repressive function during this time point[9,10]. Thus, we reasoned that an additional factor must be responsible for pri-miRNA regulation and searched our previously generated RNA-seq datasets for other abundant transcription factors. We identified E75 as a candidate transcription factor due to its high expression levels at the 72 h PE period relative to that of Kr-h1. Overexpression of E75 in our luciferase assay resulted in an induction of luciferase activity on all three of the respective candidate *pri-miRNA* promoters. E75 is conventionally thought to be an ecdysone responsive transcription factor and has largely been studied in the context of vitellogenin activation during the blood meal phase of *Ae. aegypti* female mosquitoes[11].

This reasoning could signify its exclusion from previous research experiments involved in JH regulation, despite E75 being abundant during the PE phase. Our next set of experiments are aimed at confirming the role of E75 on *pri-miRNA* regulation and deciphering the regulatory role of E75 during this critical time point in *Ae. aegypti* development.

2.6 References

1 Chen, X. & Rosbash, M. mir-276a strengthens Drosophila circadian rhythms by regulating timeless expression. *Proc Natl Acad Sci U S A* **113**, E2965-2972, doi:10.1073/pnas.1605837113 (2016).

2 Shin, S. W., Zou, Z., Saha, T. T. & Raikhel, A. S. bHLH-PAS heterodimer of methoprene-tolerant and Cycle mediates circadian expression of juvenile hormone-induced mosquito genes. *Proc Natl Acad Sci U S A* **109**, 16576-16581, doi:10.1073/pnas.1214209109 (2012).

3 Chi, S. W., Zang, J. B., Mele, A. & Darnell, R. B. Argonaute HITS-CLIP decodes microRNA-mRNA interaction maps. *Nature* **460**, 479-486, doi:10.1038/nature08170 (2009).

4 Sempere, L. F., Sokol, N. S., Dubrovsky, E. B., Berger, E. M. & Ambros, V. Temporal regulation of microRNA expression in Drosophila melanogaster mediated by hormonal signals and broad-Complex gene activity. *Dev Biol* **259**, 9-18, doi:10.1016/s0012-1606(03)00208-2 (2003).

5 Xiong, X. P. *et al.* miR-34 Modulates Innate Immunity and Ecdysone Signaling in Drosophila. *PLoS Pathog* **12**, e1006034, doi:10.1371/journal.ppat.1006034 (2016).

6 Jeong, G., Lim, Y. H. & Kim, Y. K. Precise mapping of the transcription start sites of human microRNAs using DROSHA knockout cells. *BMC Genomics* **17**, 908, doi:10.1186/s12864-016-3252-7 (2016).

7 Kayukawa, T. *et al.* Transcriptional regulation of juvenile hormone-mediated induction of Kruppel homolog 1, a repressor of insect metamorphosis. *Proc Natl Acad Sci U S A* **109**, 11729-11734, doi:10.1073/pnas.1204951109 (2012).

8 Saha, T. T. *et al.* Hairy and Groucho mediate the action of juvenile hormone receptor Methoprene-tolerant in gene repression. *Proc Natl Acad Sci U S A* **113**, E735-743, doi:10.1073/pnas.1523838113 (2016).

9 Saha, T. T. *et al.* Synergistic action of the transcription factors Kruppel homolog 1 and Hairy in juvenile hormone/Methoprene-tolerant-mediated gene-repression in the mosquito Aedes aegypti. *PLoS Genet* **15**, e1008443, doi:10.1371/journal.pgen.1008443 (2019).

10 Ojani, R., Fu, X., Ahmed, T., Liu, P. & Zhu, J. Kruppel homologue 1 acts as a repressor and an activator in the transcriptional response to juvenile hormone in adult mosquitoes. *Insect Mol Biol* **27**, 268-278, doi:10.1111/imb.12370 (2018).

11 Cruz, J., Mane-Padros, D., Zou, Z. & Raikhel, A. S. Distinct roles of isoforms of the heme-liganded nuclear receptor E75, an insect ortholog of the vertebrate Rev-erb, in mosquito reproduction. *Mol Cell Endocrinol* **349**, 262-271, doi:10.1016/j.mce.2011.11.006 (2012).

2.7 Figures and Tables

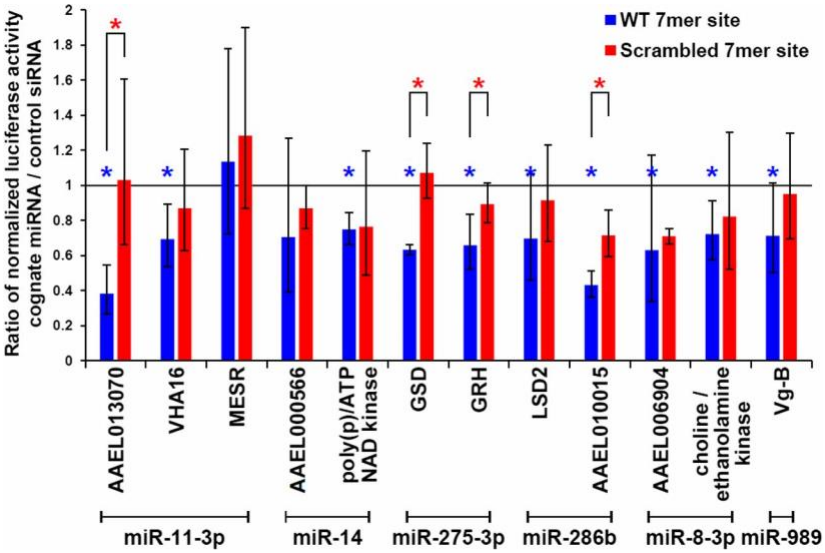

Figure 1.1: *In vitro* validation of miRNA targets generated from CLIP-Seq dataset. Relative (Renilla/Firefly activity) was measured from the wild-type (blue) and mutated (red) reporters three to five times from each candidate 3'UTR, respectively. Statistical significance was calculated using unpaired one-tailed Student's T-tests. *$P < 0.05$, Data is shown as average ± SD. Blue asterisks represent statistical significance in comparing the effect of miRNA mimic and negative control siRNA on wild-type reporters; red asterisks represent statistical significance between wild-type and mutated reporters with transfected miRNA mimic.

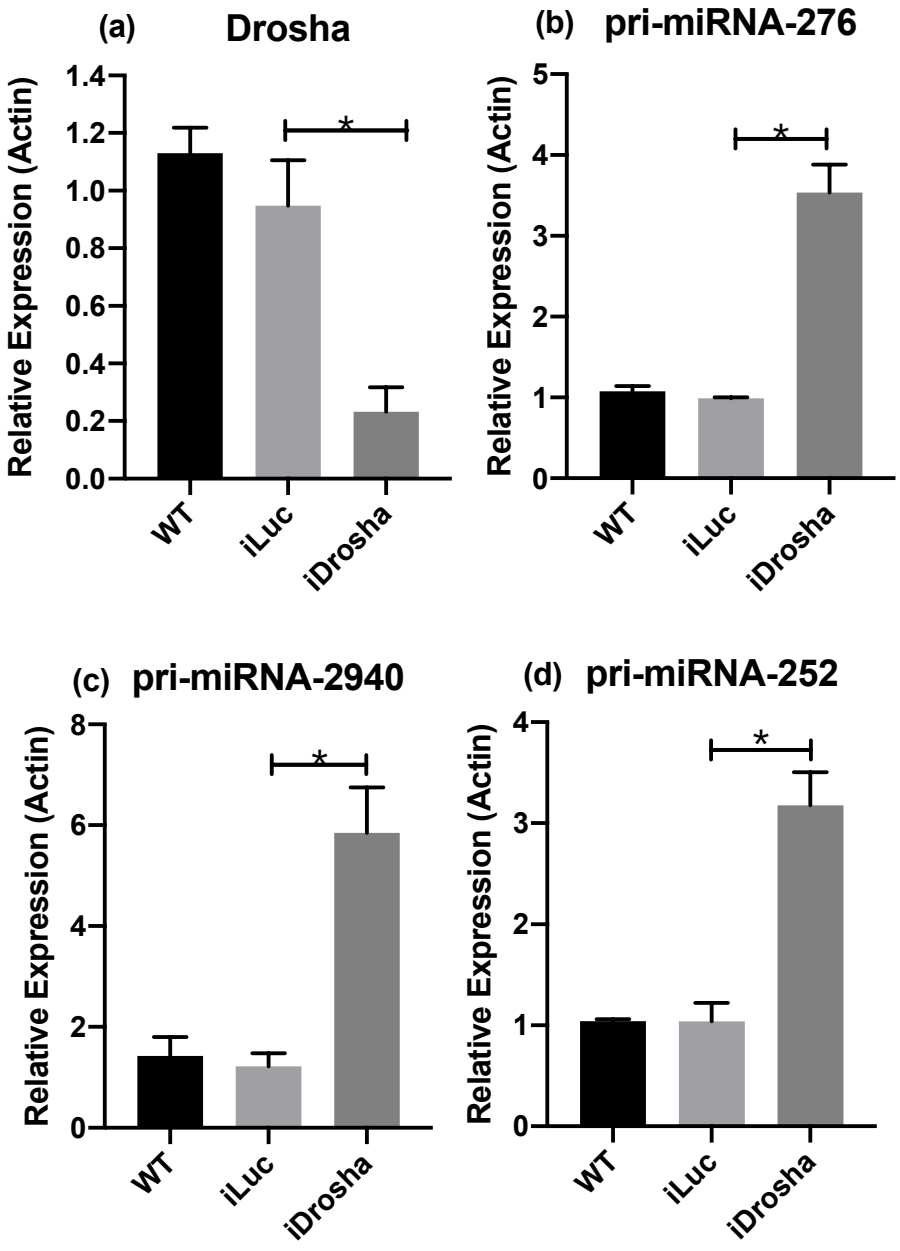

Figure 2.1: Drosha knockdown effects on pri-miRNA degradation in fat body tissue. (a). Relative gene expression levels of Drosha from fat body tissues at 72hr PE after treatment with dsRNA targeting Drosha from WT, iLuc and iDrosha groups. (b), (c) and (d), Relative gene expression levels of pri-miRNA-276, 2940 and 252, respectively, from WT, iLuc and iDrosha groups fat body tissues at 72hr PE. Each group represents an average of three independent experiments that included three to four biological samples per experiment. Statistical significance was calculated using a one-way ANOVA. *$P < 0.05$, Data is shown as average ± SEM.

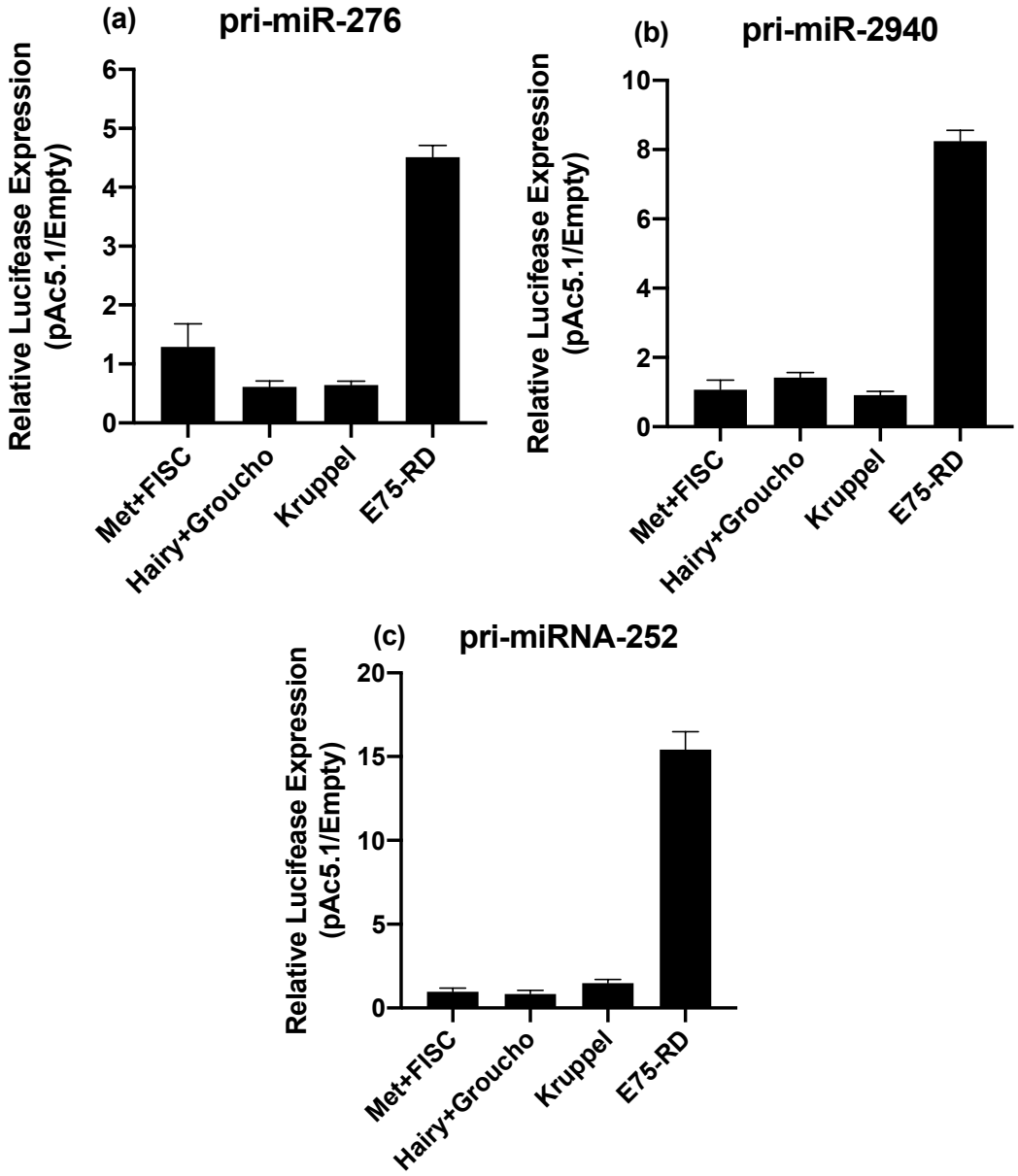

Figure 3.1 E75-RD is an activator of pri-miRNA promoters. (a), (b) and (c), Luciferase reporter assay after co-transfection with either Met and FISC, Hairy and Groucho, Kruppel or E75-RD protein expression vectors and the respective candidate pri-miRNA firefly reporter construct. Pri-miRNA promoter firefly luciferase measurements were divided by measurements from a promoter-less firefly vector and the respective candidate protein expression. Firefly luciferase measurements were then normalized to an internal *Renilla* luciferase control. Transfection experiments were completed independently three times with each experimental group having three technical replicates. Data is shown as average ± SEM.

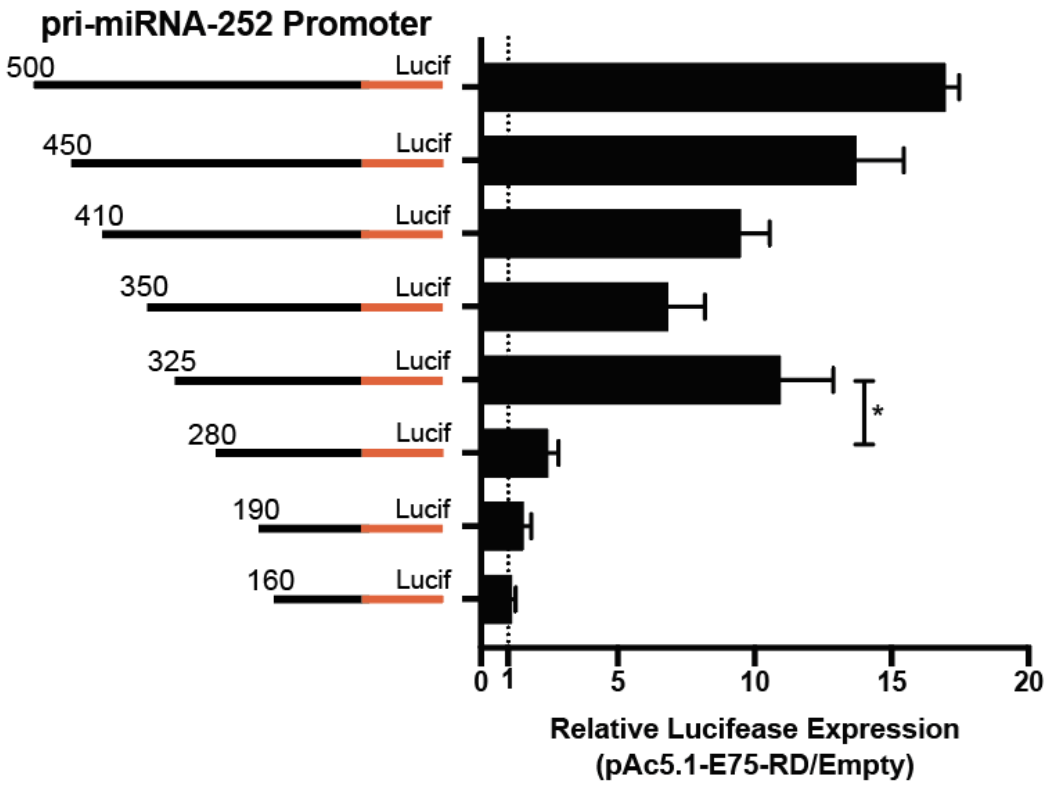

Figure 4.1. Mapping of E75-RD binding site on the pri-miRNA-252 promoter. Luciferase measurements from a serial deletion of the pri-miRNA-252 promoter with E75-RD protein expression. Firefly luciferase measurements are normalized to an internal *Renilla* luciferase control. Transfection experiments were completed independently three times with each experimental group having three technical replicates. Statistical significance was calculated using a Student's T-test. *$P < 0.05$, Data is shown as average ± SEM.

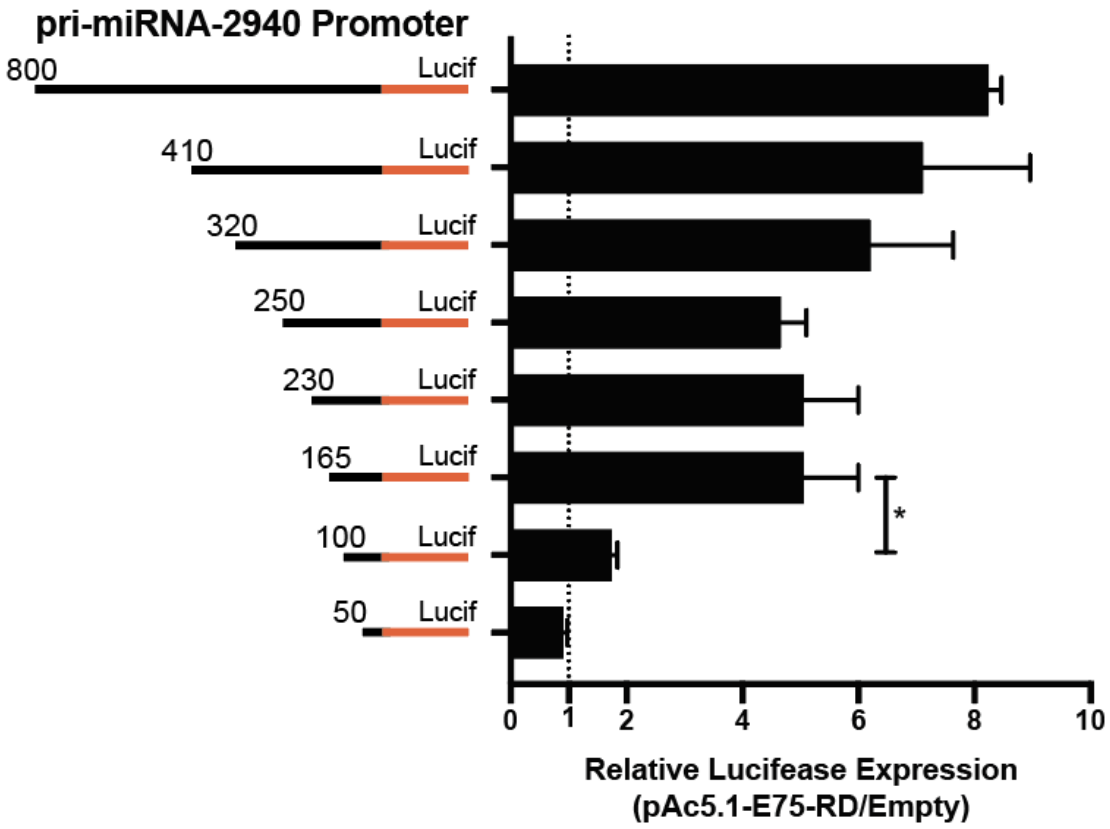

Figure 5.1. Mapping of E75-RD binding site on the pri-miRNA-2940 promoter. Luciferase measurements from a serial deletion of the pri-miRNA-2940 promoter with E75-RD protein expression. Firefly luciferase measurements are normalized to an internal *Renilla* luciferase control. Transfection experiments were completed independently three times with each experimental group having three technical replicates. Statistical significance was calculated using a Student's T-test. *$P < 0.05$, Data is shown as average ± SEM.

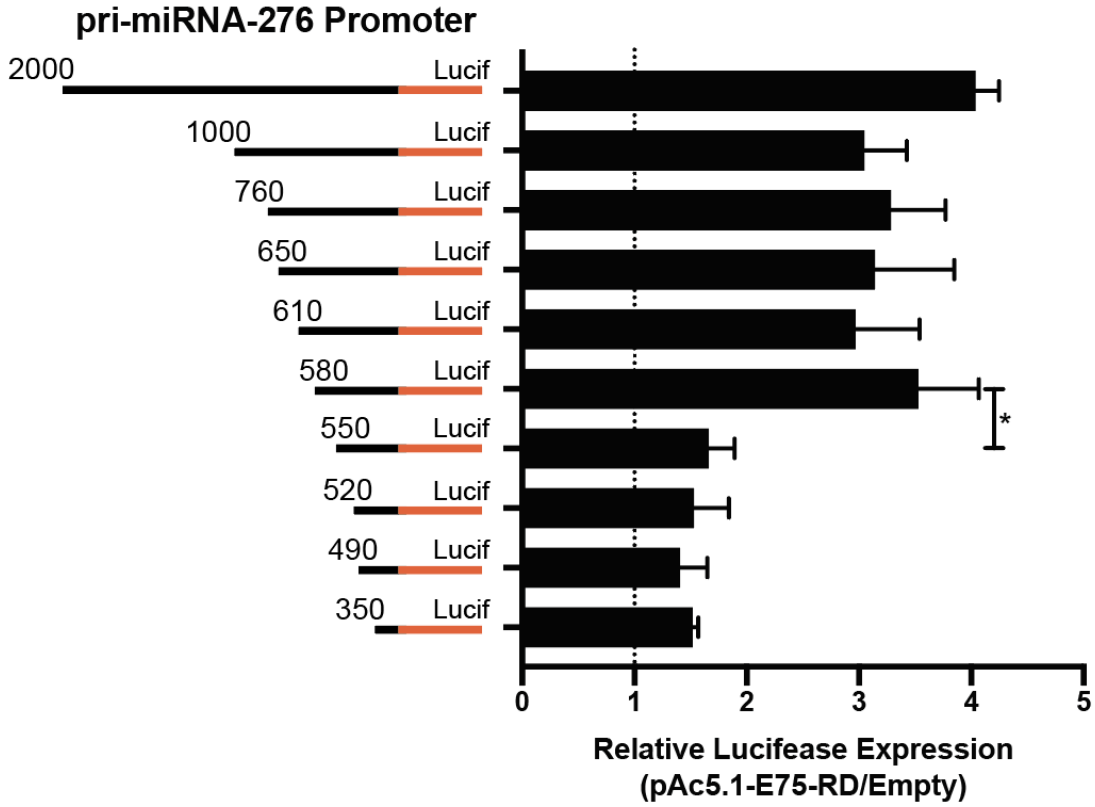

Figure 6.1. Mapping of E75-RD binding site on the pri-miRNA-276 promoter. Luciferase measurements from a serial deletion of the pri-miRNA-276 promoter with E75-RD protein expression. Firefly luciferase measurements are normalized to an internal *Renilla* luciferase control. Transfection experiments were completed independently three times with each experimental group having three technical replicates. Statistical significance was calculated using a Student's T-test. *$P < 0.05$, Data is shown as average ± SEM.

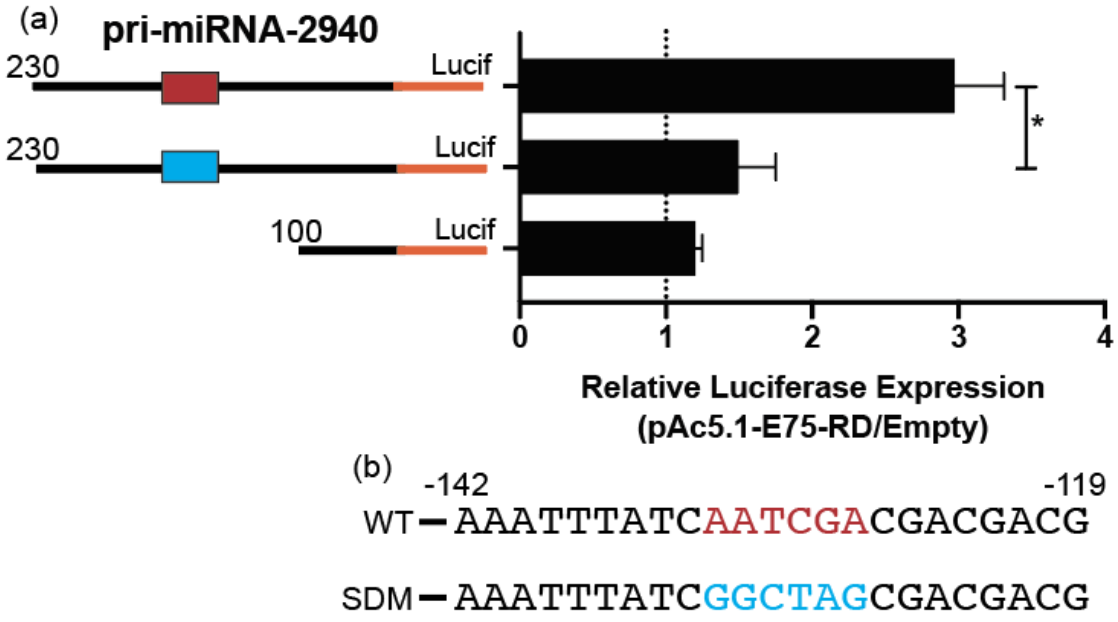

Figure 7.1. Identification of E75-RD binding site on the pri-miRNA-2940 promoter. (a), Luciferase measurements of the pri-miRNA-2940 promoter with E75-RD protein expression including a mutated sequence between 135-130 DNA region. Firefly luciferase measurements are normalized to an internal *Renilla* luciferase control. Transfection experiments were completed independently three times with each experimental group having three technical replicates. (b), Putative E75-RD binding site with flanking regions within the pri-miR-2940 promoter. The red DNA sequence corresponds to the wild-type promoter and the blue sequence corresponds to the mutations generated for the mutant promoter plasmid. Statistical significance was calculated using a Student's T-test. *P < 0.05, Data is shown as average ± SEM.

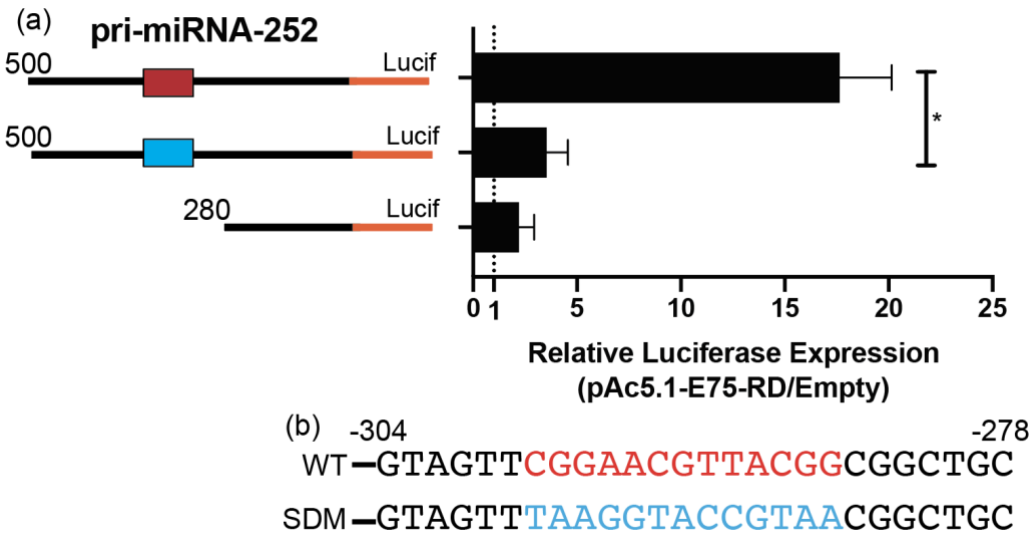

Figure 8.1. Identification of E75-RD binding site on the pri-miRNA-252 promoter. (a), Luciferase measurements of the pri-miRNA-252 promoter with E75-RD protein expression including a mutated sequence between 298-285 DNA region. Firefly luciferase measurements are normalized to an internal *Renilla* luciferase control. Transfection experiments were completed independently three times with each experimental group having three technical replicates. (b), Putative E75-RD binding site with flanking regions within the pri-miR-252 promoter. The red DNA sequence corresponds to the wild-type promoter and the blue sequence corresponds to the mutations generated for the mutant promoter plasmid. Statistical significance was calculated using a Student's T-test. *P < 0.05, Data is shown as average ± SEM.

Samples	Total Reads	Mapped Reads	% Mapped
72hr-iLuc1	45,812,628	43,043,438	94%
72hr-iLuc2	45,879,488	43,023,924	94%
72hr-iLuc3	45,673,810	43,119,686	94%
72hr-iDrosha1	46,074,566	43,359,353	94%
72hr-iDrosha2	46,369,390	43,561,743	94%
72hr-iDrosha3	47,124,122	44,597,294	95%
24hr-iLuc1	45,785,470	43,648,790	95%
24hr-iLuc2	45,579,754	43,444,065	95%
24hr-iLuc3	45,557,374	43,290,954	95%
24hr-iDrosha1	46,032,136	43,732,965	95%
24hr-iDrosha2	44,844,959	42,664,380	95%
24hr-iDrosha3	44,367,873	42,264,560	95%

Table 1.1 RNA-seq mapping statistics for the iDrosha Experiments. Total number of reads depicts the number of 2x100 Paired-End reads generated for each individual sample. The Mapped Reads are the number of reads mapped to the *Ae. aegypti* genome using HiSAT 2 program.

CHAPTER III

Assigning E75 within the Juvenile Hormone hierarchical network of gene regulation

3.1 Abstract

Our previous *in* vitro based experiments demonstrated the potential of E75 as a key transcriptional regulator of miRNA expression. Here, we confirm *in vivo* the role of E75 as part of the juvenile hormone (JH) hierarchical network, and its regulatory function as miRNA activator in the fat body tissue. The major focus of E75 research has been in the context of the ecdysone signal pathway, and as a result little information is present on the role of E75 in JH regulation. We determined that E75 transcript levels can be artificially induced by topical application of JH as well as reduced through the blockage of JH pathway by RNAi targeting of the key receptor Met. Next, we utilized small-RNA sequencing from iMet and iE75 individuals, respectively, in order to understand the global impact of E75 on miRNA expression. Lastly, we performed miRNA sequencing from the fat body tissue of iE75 individuals in an effort to characterize its functional role in the post eclosion (PE) developmental phase. Both iMet and iE75 small RNA sequencing groups display high reductions in miRNA expression, and a high overlap of similarly regulated transcripts. We also provide evidence of the transcription factor βFTZ-F1 as a potential regulator of E75. Overall, these result suggest a novel role for E75 in regulating gene expression in the fat body tissue in preparation for vitellogenin and lipid production. Our findings here establish the role of E75 in the JH hierarchical network in miRNA activation during the PE phase.

3.2 Introduction

Our prior cell culture based experiments implicated E75 as a potential transcriptional activator of miRNA expression. E75 is defined as a nuclear receptor, containing two putative zinc finger domains that function as DNA binding and ligand binding domains, respectively. E75 was originally identified as an ecdysone responsive protein in *Drosophila* larvae development[1]. Due to the positive correlation between the peaks of ecdysone titers and E75 expression during development, E75 was implicated to be part of the ecdysone regulatory pathway. The primary study on E75 function investigated the role of its three different isoforms (termed A, B and C) during the *Drosophila* life cycle[1]. Isoform-specific knockout lines were generated and monitored for phenotypic responses during development. Isoform B mutants were completely viable, showing no eminent defects. Isoform C mutants showed lethal defects during the pharate adult (33%) and adult stages (66%). The mutants that died during the pharate adult stage had no noticeable defects, however the surviving flies that emerged to the adult stage were noted as being extremely uncoordinated and died within the first week. E75A mutants had multiple developmental defects causing high lethality across multiple stages in the life cycle. E75A second instar larvae mutants were found to have lower levels of *βftz-f1* and *E74A*, indicating a deficiency in the ecdysone pathway. These mutants were found to have lower titers of 20E and provisioning 20E to these mutants by feeding restored developmental progression back to the wildtype strain. These experiments highlighted a functional role for E75A within *Drosophila* development and served as a model for studying E75 within the ecdysone signaling pathway. The above study was paramount in

linking E75 to the ecdysone signaling pathway and additional studies have further demonstrated its conservation in non-model organisms[2-4].

Previous studies in our laboratory have described E75 function during the 20E mediated blood-meal phase in the fat body tissue of *Ae. aegypti*. Individual isoforms were targeted by RNAi and examined for vitellogenin levels during the blood meal phase[5]. Each E75 isoform had a unique role in the timing and induction of *vitellogenin* expression. E75A knockdown failed to induce vitellogenin, E75B knockdown had no effect on vitellogenin abundance, while E75C knockdown resulted in higher levels of vitellogenin. The differences in the regulatory role between the E75 isoforms is thought to be related to the protein structures. E75C has two functional DNA-binding domains suggesting that its capable of regulating gene expression. E75A/B have one functional DNA-binding domain and as a result will bind to co-receptor HR3 to regulate gene expression[6].

Due to the 20E effect on E75, this transcription factor has been solely portrayed as an ecdysone regulatory protein. However, a few studies indicate the possibility that E75 could be regulated by juvenile hormone. In the initial study, *Drosophila* S2 cells were treated with JH III and a large induction of only E75A was observed over a two-hour period[7]. A follow up study examined the role of βFTZ-f1 as a transcriptional regulator of E75A after JH III treatment in *Drosophila* S2 cells[8]. βFTZ-f1 is a DNA-binding transcription factor that has been shown to be induced after the ecdysteroid pulse at the mid-prepupal stage of development and result in the induction of E75A[8]. Knockdown of βFTZ-f1 through RNAi treatment prevented the induction of E75A after JH III treatment, suggesting that it may be a regulatory factor controlling E75A expression. Overexpression

of βFTZ-f1 protein resulted in induction of the E75A promoter in a luciferase based experiment and co-immunoprecipitation of βFTZ-f1 found that it bound to the region upstream of the E75A promoter[8]. Both of these experiments highlighted the functional role of βFTZ-f1 as a transcriptional regulator of E75A.

Our prior *in vitro* promoter analysis based experiments specifically implicated the role of E75-RD (originally termed E75C in *Drosophila*) in miRNA activation in *Ae. aegypti*. E75-RD was identified based on the isoform specific expression profile during the PE developmental stage. While the other three isoforms (E75-A, -B and -D) are expressed during the blood meal phase, only E75-RD is expressed at the PE stage[9]. In the work described in this chapter, we demonstrate that E75 is part of the juvenile hormone hierarchical network and characterize the functional role of E75 in the fat body tissue during the PE developmental stage for egg development.

3.3 Material and Method

Juvenile hormone *in vivo* application

Newly emerged female mosquitoes (3hr PE) were collected and chilled on ice and a 0.3-μL aliquot of 1 μg/mL JH III (Sigma) or solvent (acetone) was topically applied to the abdomen. Fat body tissue (~5-6 per biological replicate) was collected 6 h post-treatment and subjected to RNA extraction and RT-qPCR as described below.

Double-stranded RNAi injections

DsRNA for *iLuc*, *iMet*, *iE75com* and *iβftz-f1* was synthesized using the MEGAscript Kit (Ambion). At 12hr PE, 0.5µg (.25µl of 2µg/µl) dsRNA was injected into the thorax of adult female mosquitoes. Mosquitoes were allowed to recover for 3-4 days on both H_20 and sugar water before dissection and fat body tissue collection.

Quantitative Reverse Transcription PCR (qRT-PCR)

Total RNA was prepared using Trizol (Invitrogen) following the standard protocol. Total RNA was purified using Zymo RNA cleanup kit (R1018) and in-column DNase treatment (E1010). Total RNA was quantified using Nanodrop 2000 and 2.5µg was subjected to cDNA synthesis using the SuperScript III Kit (Invitrogen). Expression data was plotted as $2^{-\Delta Ct}$ whereby the cycle threshold (Ct) for the gene of interest is compared with the Ct of the internal control gene. All expression data are plotted as relative expression to *actin*.

RNA-seq Analysis

Total RNA was sent UCR Gencore for next-generation sequencing on the illumina NextSeq 550. mRNA was isolated by poly-A tail pulldown and used for cDNA synthesis. Library preparation was completed under their protocol. Paired reads were mapped to the *Ae. aegypti* Genome (AaegL5.1) using HISAT. Afterwards, reads were separated based on whether or not they matched to the current *Ae. aegypti* transcriptome reference using Bedtools. For reads that mapped to the *Ae. aegypti* transcriptome, transcript abundance

(FPKM) was estimated using Stringtie and differential expression analysis was completed using Ballgown. For reads that did not match to *Ae. aegypti* transcripts, reads from all samples were concatenated together and used for assembly of novel transcripts in Stringtie. Library depth and mapping statistics for individual libraries are included in Table 1.1. FPKM were estimated for individual samples against the newly generated reference of novel transcripts and differential expression analysis was completed using Ballgown.

Small RNA library preparation and analysis

3µg of total RNA was run on a Novex TBE-Urea 15% (Invitrogen) at 100V for 1 hr. The gel was stained with SYBR Gold for 10 minutes and visualized under UV light. The portion containing small RNAs was excised with a razor and purified using ZR small-RNA PAGE recovery kit (Zymo). Confirmation of small RNAs was completed using small RNA bioanalyzer chip (Agilent) and used for the small RNA library prep kit (NEB). Library preparation followed manufacturer's protocol without any changes. Small RNA reads were trimmed to 18 basepairs (fastx-tool kit) and mapped to *Ae. aegypti* genome allowing 1 mismatch (bowtie). Mapped reads were counted using HT-Seq and differential expression analysis was completed using EdgeR. Library depth and mapping statistics for individual libraries are included in Table 1.2.

3.4 Results

As E75 is largely thought to be an ecdysone responsive gene, we first set out to establish its role within the JH hierarchical network. Two preliminary experiments were

completed to support the hypothesis that E75 is regulated by JH. Topically applying JH to the abdomen of newly eclosed adult mosquitoes can result in an artificial activation of JH pathway in the fat body tissue[10]. Accordingly, we topically applied JH III to the abdomen of female mosquitoes 0-3 h PE and 6 h posttreatment dissected fat body tissues. We analyzed *E75-RD* expression and noted that fat body samples treated with JH III had elevated gene expression levels compared to the acetone treatment alone and wild type controls, respectively (Figure 1.1). Next, we performed RNAi on Met, the key hormonal receptor for JH activation. Removal of Met through dsRNA knockdown has been shown to be an effective method to prevent JH activation, blocking both the induction of Hairy and Kr-h1[11]. We reasoned that *E75-RD* would also display a decreased expression level in the absence of Met. We injected adult female mosquitoes 0-24 h PE with dsRNA targeting either *met* (iMet) or *luciferase* (iLuc) and subsequently measured *E75-RD* expression levels in the fat body tissue 4 d later. Upon treatment with iMet, we found that *E75-RD* was reduced in the fat body in comparison to the iLuc control group (Figure 2.1).

Previous experiments connecting Hairy to the JH network utilized RNA-seq analysis from the fat body tissues of iMet and iHairy treatment groups, respectively. Approximately 79% of the genes up-regulated in the iHairy group were also found to be up-regulated in the iMet group[10]. This high intersection of gene expression profile suggests that Hairy is a likely regulatory factor downstream of Met in the JH pathway. We next performed a similar conceptual experiment; however, utilized small RNA sequencing instead of mRNA-seq analysis. We purified total RNA from iLuc, iMet and iE75 fat body samples, and prepared small RNA libraries for next generation sequencing, respectively.

Three independent biological samples from each treatment group were used for the differential expression analysis. We examined the global small RNA profile (tRNA, rRNA, pre-miRNA, lncRNAs, and snRNAs) and found large expression changes in the iMet and iE75 groups in comparison to the iLuc control. Interestingly, the proportion of reads mapping to rRNAs, lcnRNAs, snRNAs and tRNAs increased in the iMet and iE75 groups, while the proportion related to pre-miRNAs decreased in both treatment groups (Figure 3.1). Approximately 55% of the genes were upregulated in both the iMet and iE75 groups when compared to the iLuc, while about 73% were downregulated in both treatment groups relative to control, respectively (Figure 4.1). Interestingly the down-regulated set of genes contained 40 out of the 52 miRNAs, with the remaining 12 miRNAs not differentially expressed and being expressed on the low end of detection (Figure 5.1 and 5.2). Specifically, the f.c. for *miR-276, miR-252* and *miR-2940* was found to be .42, .45 and .53 respectively. This finding supports our previous cell cultured based experiments, further suggesting the role of E75-RD as an activator of miRNA expression.

Since there was a high correlation between the genes effected by iMet and iE75, we set out to investigate whether Met is a direct activator of E75-RD. We cloned the ~1100bp region upstream of E75-RD start site, and tested its ability to induce luciferase expression in the cell culture based assay. There was no change in luciferase levels with the addition of pAc5.1-Met and pAc5.1-FISC protein expression vectors, implying that while Met has an impact on *E75-RD* expression, it is not a direct regulator. Since βFTZ-f1 had been previously connected to *E75A* regulation in *Drosophila*, we speculated that this regulatory network could be conserved in *Ae. aegypti*, albeit now shifted to function for

the *E75-RD* isoform. βFTZ-f1 has previously been described as a JH inducible gene in *Ae. aegypti* and critical for recruiting EcR/USP to the vitellogenin promoter during the ecdysone phase[12]. We performed RNAi targeting βFTZ-f1 and subsequently measured gene expression levels for E75-RD. Interestingly, we noted a ~40% reduction in E75-RD gene expression levels; however, there was only a ~20% reduction other JH inducible transcription factors Kr-h1 and Hairy (Figure 6.1). This finding is contrary to iMet treatment which negatively impacts the expression of all three transcription factors. This led us to believe that βFTZ-f1 is specifically responsible for regulating E75-RD. However, when we performed the luciferase assay with the E75-RD putative promoter *in vitro* by adding βFTZ-f1 and Taiman (FISC), we did not note any increase in luciferase production. It is possible that the DNA binding site for βFTZ-f1 could be located further up-stream than the 1100 bp region we analyzed as the putative promoter region of E75-RD.

We performed RNA-seq analysis from iE75 and iβFTZ-f1 to examine the global regulator impact of these two transcriptional factors on fat body development. The RNA-seq data verified our previous RT-qPCR findings where iβFTZ-f1 impacted E75 specifically, having no impact Kr-h1 and Hairy transcript levels. (Table 2.1). We first compared overall changes in gene expression in a similar manner to the previous small RNA analysis we performed with iE75 and iMet. We found that ~ 34% of genes up-regulated and ~33% of genes down-regulated were shared between the iE75 and iβFTZ-f1 datasets (Figure 7.1). We applied GO-Term analysis to broadly identify functional changes occurring in the fat body in the absence of βFTZ-f1 and E75, respectively. For iβFTZ-f1, up-regulated terms were largely associated with "DNA replication", "mitochondrial

activity" and "serine-type endopeptidase activity", while down-regulated terms were largely associated with “membrane bound proteins” and "transmembrane transport" (Table 3.1 and 3.2). For iE75, up-regulated terms were largely associated with "proteolysis", "serine-type endopeptidase activity" and "plasma membrane", while down-regulated terms were associated with "extracellular region" and "lipid particles" (Table 4.1 and 4.2). The next investigation of our study will explore whether E75 mediated activation of miRNAs is responsible for regulating reproductive physiology in this critical stage.

3.5 Discussion

E75 has largely been characterized as an ecdysone responsive transcription factor. Here, we describe an E75 isoform under the regulation of juvenile hormone in the fat body tissue of *Ae. aegypti*. We establish that the E75-RD isoform is regulated indirectly by the Met receptor and is part of the juvenile hormone hierarchical network. Although we have not identified the direct regulator, we provide evidence that βFTZ-f1 is involved in the regulation of E75-RD. βFTZ-f1 has been shown to be regulated through JH III action and is an important competence factor for vitellogenin activity[13]. The overlapping set of up- and down-regulated genes we identified in the RNA-seq analysis comparing iβFTZ-f1 and iE75 treatments were consistent within the two datasets. The ~33% of the transcripts we found to be similarly regulated is consistent with our previous experiments performed for iHairy and iKr-H1 treatments, indicating that βFTZ-f1 and E75 are in a shared network. Although our luciferase promoter assay for E75-RD did not indicate any direct binding for βFTZ-f1 to the promoter region, it is possible that the putative region we examined did not

span upstream enough to contain the βFTZ-f1 binding site. The *Drosophila* experiments that demonstrated βFTZ-f1 as a regulator of the JH inducible E75A found the location of βFTZ-f1 binding site to be ~5kb upstream of the E75A promoter[8]. Additional ChIP-seq experiments targeting βFTZ-f1 would be insightful in locating the direct binding site for the E75-RD promoter.

Using RNA-seq analysis from iE75 samples, we set out to characterize the functional role of E75 during the PE phase. From our GO term analysis, genes associated with “serine proteases function” increased in iE75, while genes involved in “lipid particles and membrane association” decreased. Specifically, we saw an increase in a few midgut-specific trypsin and chymotrypsin genes (AAEL001703, AAEL003060 and AAEL007818) that have peak transcriptional activity during the PE stage[14,15]. None of the remaining genes associated with "serine protease function" have been associated with digestive-enzymes abundant in the midgut the during blood feeding stage[14]. Our prior studies have demonstrated the regulation of early trypsin to be mediated through Met and juvenile hormone activation[16]. The up-regulation of trypsin/chymotrypsin has also been noted in a recent study examining RNA-seq data from Met KO in *Aedes* L4 larvae[17]. Thus, it is likely the genes associated "serine protease function" described here have an alternative function beside midgut digestion. The upregulation of these transcripts could be a defect resulting from the dysfunction of a specific development process tied to the activity of the cellular membrane.

Our previous luciferase based promoter analysis, described in Chapter 2, implicated E75-RD as an activator of miRNA expression for *pri-miR-276, pri-miR-2940* and *pri-miR-*

252. The small RNA-seq analysis from both iMet and iE75 samples indicated large global changes to the small RNA profile in the fatb ody tissue. Both samples indicated a major decrease in miRNA expression, with iE75 having a larger reduction effect on miRNAs than iMet. Although our previous results demonstrated E75-RD as an activator of above mentioned miRNA, it is unlikely that E75-RD is a direct regulator of all miRNAs. E75-RD likely contributes to fat body development, and thus, in its absence, a particular process may be inhibited contributing to the global decrease of miRNA expression noted in our analysis. Our next set of experiments are aimed at understanding the role of E75-RD in miRNA activation in the fat body tissue during this phase. We aim to explore whether the miRNAs, regulated by E75-RD are critical to a process required for reproduction. Synthetic RNA probes, termed antagomirs, will be utilized to experimentally block individual miRNAs, *miR-252, miR-2940* or *miR-276*, respectively. We will then screen the antagomir treated individuals for proper primary ovarian follicle development and egg production post blood meal feeding. The candidate miRNA(s) responsible for the reproductive defect will be examined for its molecular target. This information will provide insight into the specific process disrupted. *In silico* miRNA-mRNA target predictions will be completed and validated *in vitro* through a luciferase based cell culture assay and *in vivo* by measuring changes in gene expression by RT-qPCR from knockdown individuals. Identifying the mRNA target will enable a deeper understanding of the specific biological processes regulated by miRNAs for fat body development during the PE phase.

3.6 References

1 Segraves, W. A. & Hogness, D. S. The E75 ecdysone-inducible gene responsible for the 75B early puff in Drosophila encodes two new members of the steroid receptor superfamily. *Genes Dev* **4**, 204-219, doi:10.1101/gad.4.2.204 (1990).

2 Keshan, B., Hiruma, K. & Riddiford, L. M. Developmental expression and hormonal regulation of different isoforms of the transcription factor E75 in the tobacco hornworm Manduca sexta. *Dev Biol* **295**, 623-632, doi:10.1016/j.ydbio.2006.03.049 (2006).

3 Kamae, Y., Uryu, O., Miki, T. & Tomioka, K. The nuclear receptor genes HR3 and E75 are required for the circadian rhythm in a primitive insect. *PLoS One* **9**, e114899, doi:10.1371/journal.pone.0114899 (2014).

4 Li, K. *et al.* Bombyx E75 isoforms display stage- and tissue-specific responses to 20-hydroxyecdysone. *Sci Rep* **5**, 12114, doi:10.1038/srep12114 (2015).

5 Cruz, J., Mane-Padros, D., Zou, Z. & Raikhel, A. S. Distinct roles of isoforms of the heme-liganded nuclear receptor E75, an insect ortholog of the vertebrate Rev-erb, in mosquito reproduction. *Mol Cell Endocrinol* **349**, 262-271, doi:10.1016/j.mce.2011.11.006 (2012).

6 Reinking, J. *et al.* The Drosophila nuclear receptor e75 contains heme and is gas responsive. *Cell* **122**, 195-207, doi:10.1016/j.cell.2005.07.005 (2005).

7 Dubrovsky, E. B., Dubrovskaya, V. A. & Berger, E. M. Hormonal regulation and functional role of Drosophila E75A orphan nuclear receptor in the juvenile hormone signaling pathway. *Dev Biol* **268**, 258-270, doi:10.1016/j.ydbio.2004.01.009 (2004).

8 Dubrovsky, E. B. *et al.* The Drosophila FTZ-F1 nuclear receptor mediates juvenile hormone activation of E75A gene expression through an intracellular pathway. *J Biol Chem* **286**, 33689-33700, doi:10.1074/jbc.M111.273458 (2011).

9 Cruz, J., Sieglaff, D. H., Arensburger, P., Atkinson, P. W. & Raikhel, A. S. Nuclear receptors in the mosquito Aedes aegypti: annotation, hormonal regulation and expression profiling. *FEBS J* **276**, 1233-1254, doi:10.1111/j.1742-4658.2008.06860.x (2009).

10 Saha, T. T. *et al.* Hairy and Groucho mediate the action of juvenile hormone receptor Methoprene-tolerant in gene repression. *Proc Natl Acad Sci U S A* **113**, E735-743, doi:10.1073/pnas.1523838113 (2016).

11 Zou, Z. *et al.* Juvenile hormone and its receptor, methoprene-tolerant, control the dynamics of mosquito gene expression. *Proc Natl Acad Sci U S A* **110**, E2173-2181, doi:10.1073/pnas.1305293110 (2013).

12 Zhu, J., Chen, L., Sun, G. & Raikhel, A. S. The competence factor beta Ftz-F1 potentiates ecdysone receptor activity via recruiting a p160/SRC coactivator. *Mol Cell Biol* **26**, 9402-9412, doi:10.1128/MCB.01318-06 (2006).

13 Zhu, J., Chen, L. & Raikhel, A. S. Posttranscriptional control of the competence factor betaFTZ-F1 by juvenile hormone in the mosquito Aedes aegypti. *Proc Natl Acad Sci U S A* **100**, 13338-13343, doi:10.1073/pnas.2234416100 (2003).

14 Li, X. *et al.* Serine hydroxymethyltransferase controls blood-meal digestion in the midgut of Aedes aegypti mosquitoes. *Parasit Vectors* **12**, 460, doi:10.1186/s13071-019-3714-2 (2019).

15 Lucas, K. J., Zhao, B., Roy, S., Gervaise, A. L. & Raikhel, A. S. Mosquito-specific microRNA-1890 targets the juvenile hormone-regulated serine protease JHA15 in the female mosquito gut. *RNA Biol* **12**, 1383-1390, doi:10.1080/15476286.2015.1101525 (2015).

16 Li, M., Mead, E. A. & Zhu, J. Heterodimer of two bHLH-PAS proteins mediates juvenile hormone-induced gene expression. *Proc Natl Acad Sci U S A* **108**, 638-643, doi:10.1073/pnas.1013914108 (2011).

17 Zhu, G. H., Jiao, Y., Chereddy, S., Noh, M. Y. & Palli, S. R. Knockout of juvenile hormone receptor, Methoprene-tolerant, induces black larval phenotype in the yellow fever mosquito, Aedes aegypti. *Proc Natl Acad Sci U S A* **116**, 21501-21507, doi:10.1073/pnas.1905729116 (2019).

3.7 Figures and Tables

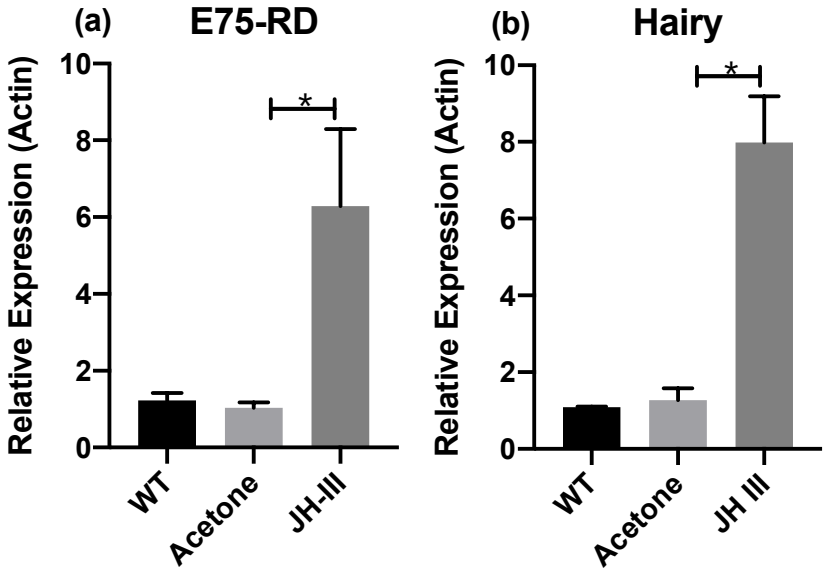

Figure 1.1 *In vitro* application of JH III impacts E75 and Hairy. (a) and (b), Relative gene expression levels of E75-RD and Hairy from WT, Acetone and JH III treated fatb ody tissues dissected at 6 hrs post treatment, respectively. Each group is the average from three independent experiments that included three to four biological samples per experiment. Statistical significance was calculated using a one-way ANOVA. *$P < 0.05$, Data is shown as average ± SEM.

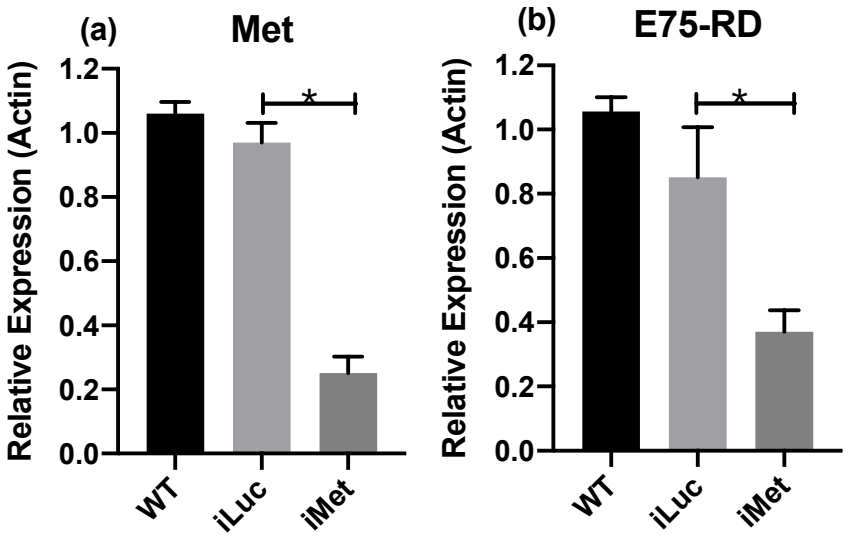

Figure 2.1. RNAi treatment of Met reduces expression of isoform E75-RD. (a) and (b), Relative gene expression levels of Met and E75-RD from WT, iLuc and iMet from fat body tissues dissected at 72hr PE. Each group is the average from three independent experiments that included three to four biological samples per experiment. Statistical significance was calculated using a one-way ANOVA. *$P < 0.05$, Data is shown as average ± SEM.

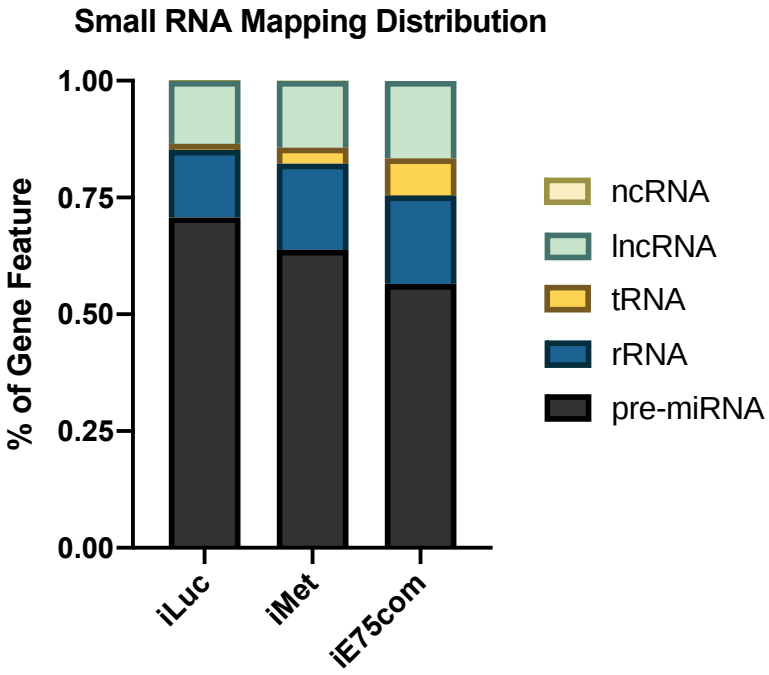

Figure 3.1. Relative abundance of non-coding RNAs from Small RNA-seq analysis. The relative abundance of non-coding (nuclear RNAs, long non-coding RNAs, transfer RNAs, ribosomal RNAs and pre-miRNAs) from the iLuc, iMet and iE75com small RNA-seq dataset.

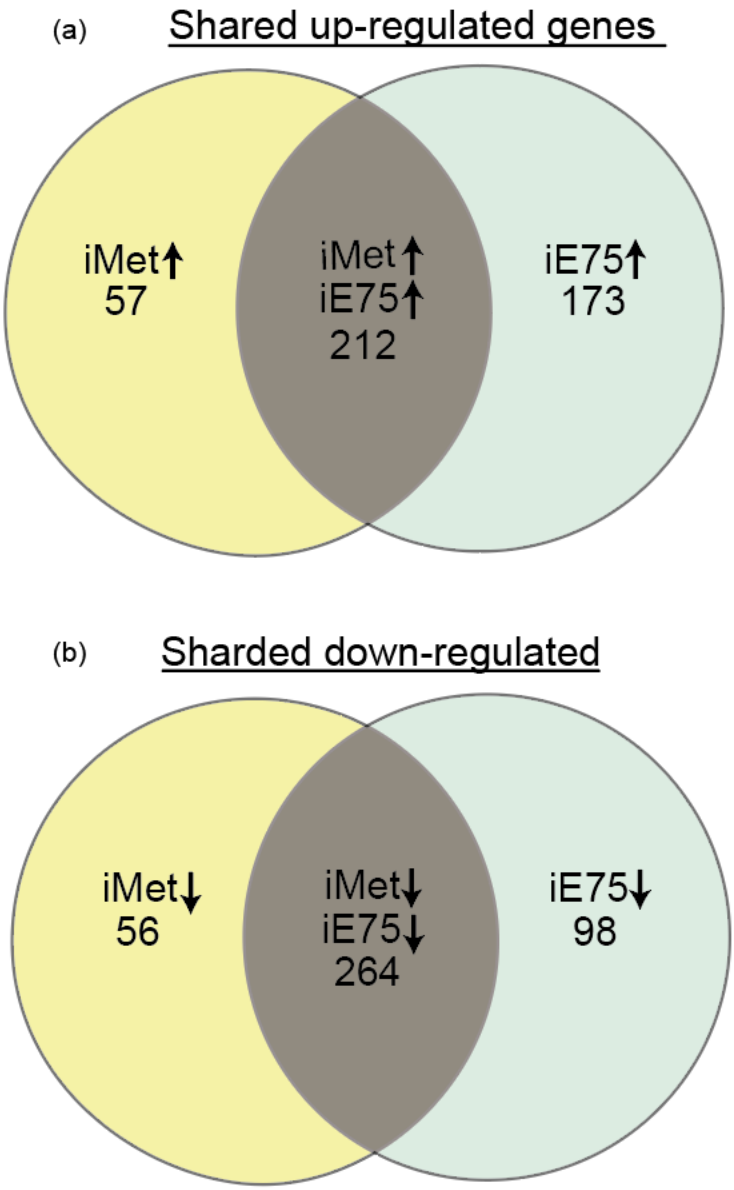

Figure 4.1 Venn diagram analysis Met and E75 RNAi Small RNA-sequencing analysis. 55% and 77% of the genes were up-down regulated in both the iMet and iE75 groups, respectively.

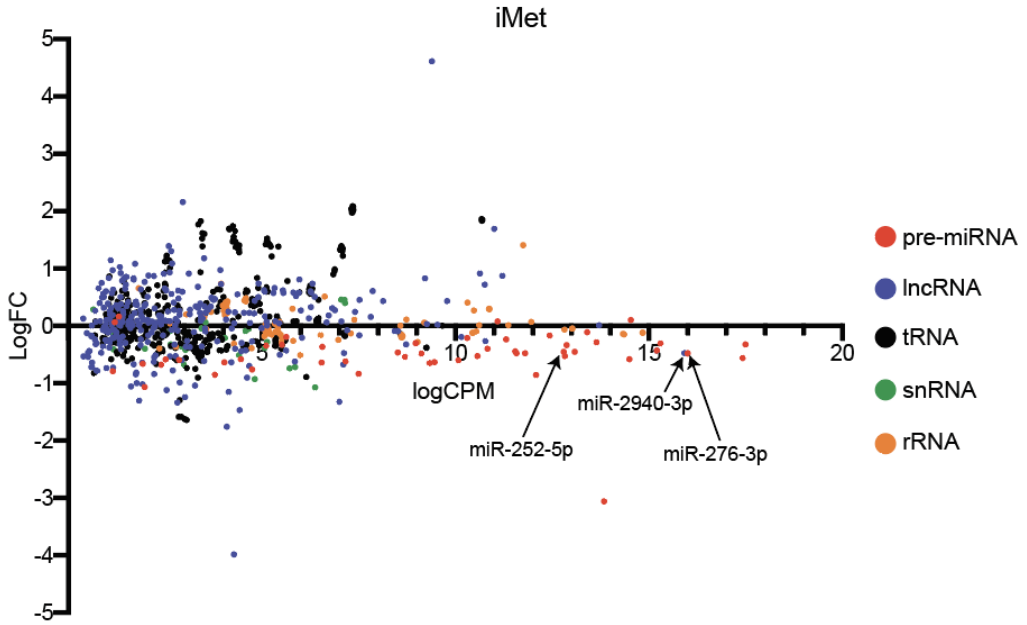

Figure 5.1. M-A plot depicting Small-RNA sequencing results from iMet analysis. X-axis represents the fold change and the Y-axis represents the mean average (counts-per-million) between the iLuc and iMet samples. Each point is representative of an individual gene and the different colors represent different classes of non-coding RNAs.

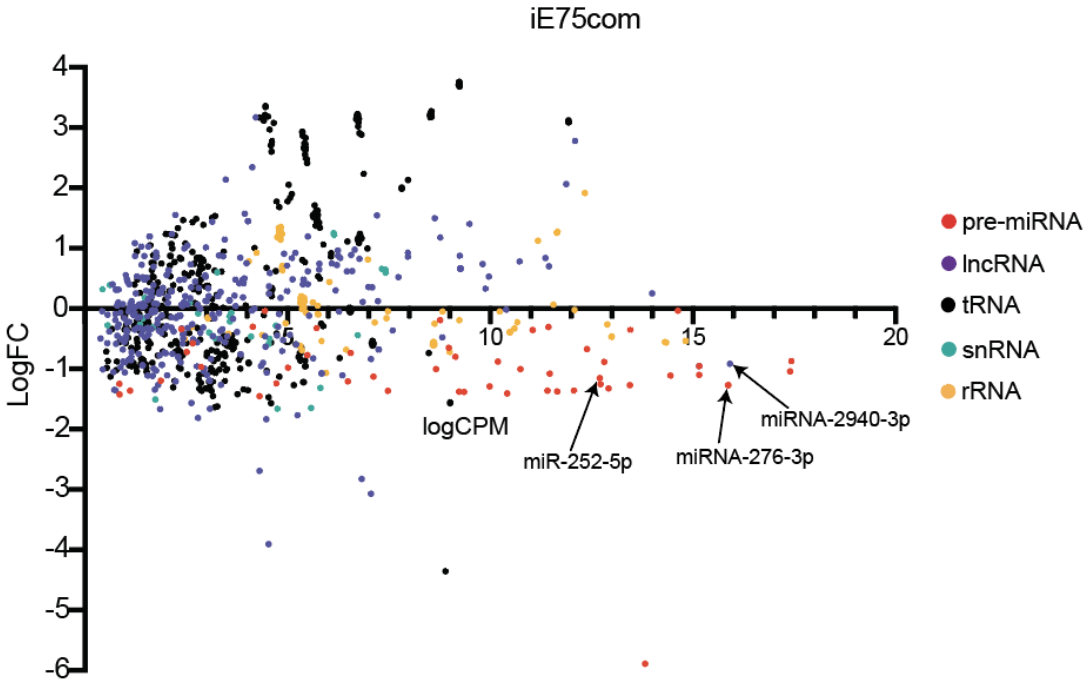

Figure 5.2. M-A plot depicting Small-RNA sequencing results from iE75com analysis. X-axis represents the fold change and the Y-axis represents the mean average (counts-per-million) between the iLuc and iE75com samples. Each point is representative of an individual gene and the different colors represent different classes of non-coding RNAs.

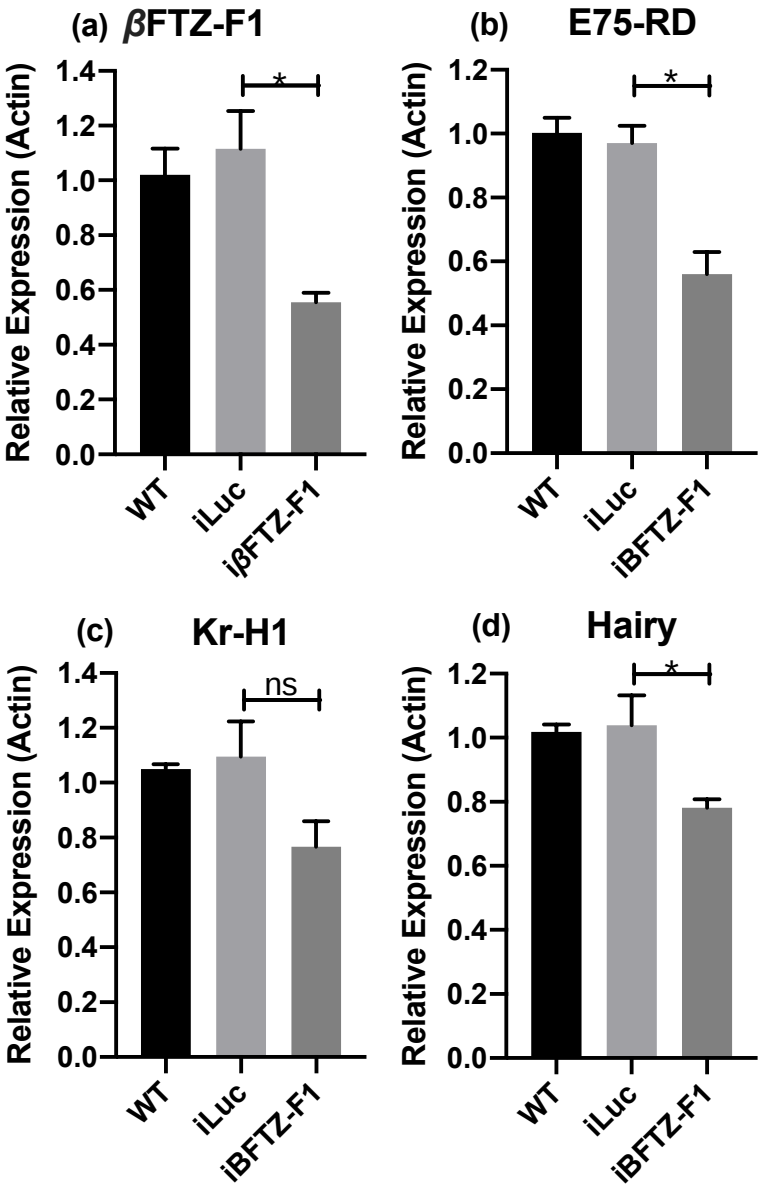

Figure 6.1. βFTZ-F1 knockdown impacts E75-RD expression in the fat body tissue. (a). Relative gene expression levels of βFTZ-F1 after treatment with dsRNA targeting βFTZ-F1 from WT, iLuc and βFTZ-F1 groups fat body tissues at 72hr PE. (b), (c) and (d), Relative gene expression levels from E75-RD, Kr-H1 snd Hairy, respectively, from WT, iLuc and βFTZ-F1 groups fat body tissues at 72hr PE. Each group is the average from three independent experiments that included three-four biological samples per experiment. Statistical significance was calculated using a one-way ANOVA. *$P < 0.05$, Data is shown as average ± SEM.

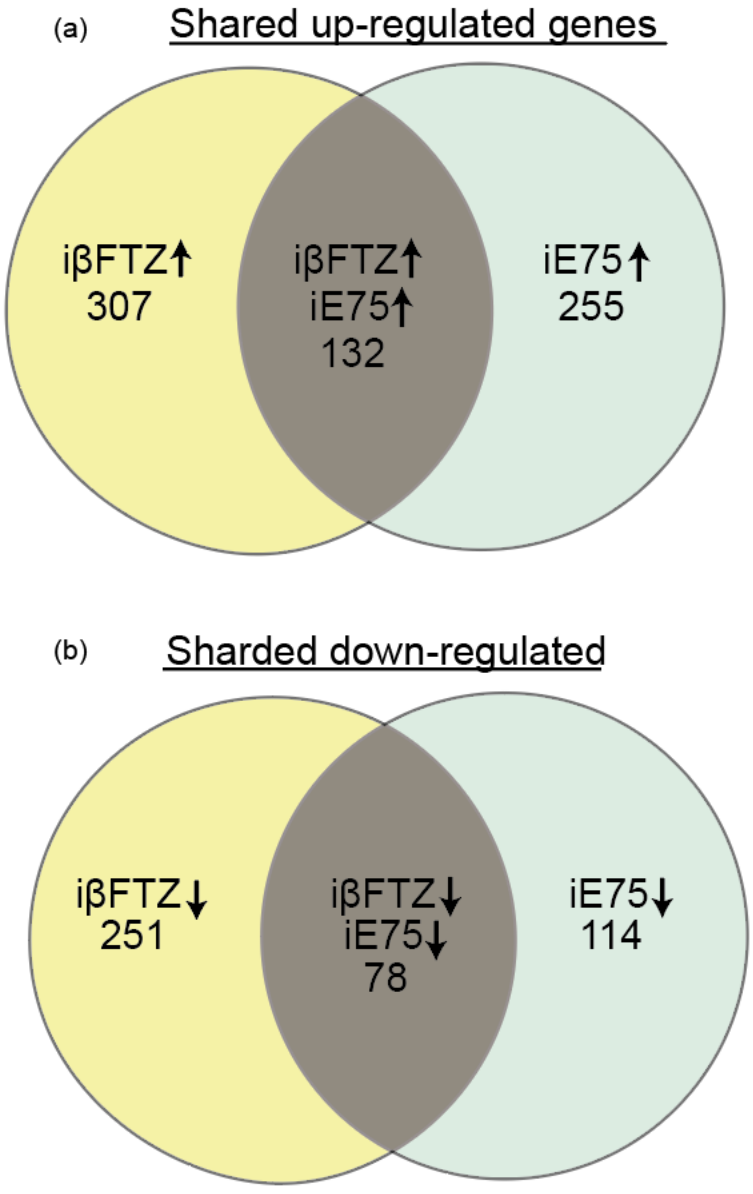

Figure 7.1. Venn diagram analysis βFTZ-F1 and E75 RNAi transcriptome. 34% and 33% of up/down-regulated genes are shared between dsβFTZ-f1 and dsE75 RNAi data sets.

Samples	Total Number	Mapped	%
iLuc1	26,546,599	23,162,263	87%
iLuc2	53,457,950	47,448,350	89%
iLuc3	51,483,324	46,206,696	90%
iE75-1	42,426,457	38,472,682	91%
iE75-2	40,548,470	36,681,589	90%
iE75-3	55,316,624	50,160,889	91%
iβFTZ-1	59,051,391	53,165,201	90%
iβFTZ-2	61,138,140	55,218,120	90%
iβFTZ-3	31,457,028	27,038,265	86%

Table 1.1 RNA-seq mapping statistics for the iβFTZ-F1 and iE75 Experiments. Total number of reads depicts the number of 1x100 Single-End reads generated for each individual sample. The Mapped Reads are the number of reads mapped to the *Ae. aegypti* genome using HiSAT 2 program.

Name	Total #	Mapped #	mRNA	pre-miRNA	rRNA	tRNA	lncRNA	snRNA	Unassigned
iLuc1	39,956,385	35,579,058	3,793,378	9,160,038	2,712,859	260,222	2,182,102	3,462	4,377,327
iLuc2	37,589,213	32,351,505	4,102,140	12,057,249	1,836,564	174,270	1,917,451	2,737	5,237,708
iLuc3	27,719,089	24,751,555	3,046,130	8,996,597	1,572,334	120,614	1,624,162	2,069	2,967,534
iMet-1	36,114,922	32,392,966	3,879,855	5,658,764	2,584,610	603,713	1,409,451	2,578	3,721,956
iMet-2	36,163,439	32,660,181	4,106,474	11,901,897	1,782,904	181,926	2,158,532	2,661	3,503,258
iMet-3	34,918,188	31,654,285	3,551,205	6,952,495	2,156,166	370,047	1,755,235	2,404	3,263,903
iE75-1	40,382,030	35,934,563	4,391,349	6,767,929	1,947,234	1,048,514	2,162,336	1,962	4,447,467
iE75-2	30,909,058	28,087,268	3,437,782	4,977,982	2,100,895	733,969	1,443,650	2,535	2,821,790
iE75-3	32,072,997	29,439,126	3,660,821	5,824,133	1,742,574	704,831	1,574,425	2,516	2,633,871

Table 1.2 Small RNA sequencing mapping results for iMet and iE75. Each row depicts a single library and the columns represent the number of reads that mapped to that specific "gene feature" using the bioinformatic program featureCounts. Ambiguous reads with the potential to map to multiple genes were not counted.

(a)

Gene ID	Flybase	Annotation	Fold change
AAEL002390	FBgn0266450	Kr-h1	1.020
AAEL027674	FBgn0001168	Hairy	1.192
AAEL007397	FBgn0000568	Eip75B	0.462
AAEL019863	FBgn0001078	ftz-f1	1.109

(b)

Gene ID	Flybase	Annotation	Fold change
AAEL002390	FBgn0266450	Kr-h1	0.9935
AAEL027674	FBgn0001168	Hairy	1.1063
AAEL007397	FBgn0000568	Eip75B	0.6702
AAEL019863	FBgn0001078	ftz-f1	0.7635

Table 2.1. Fold change for Juvenile Hormone transcription factors from iE75 and iβFTZ-F1 RNA-Seq datasets. (a) and (b) Fold change for Kr-H1, Hairy, E75 and βFTZ-F1 from iE75 and βFTZ-F1 RNA-seq datasets, respectively. The Gene ID represents the AAEL annotation from Vectorbase, the Flybase ID corresponds to the Drosophila Homolog annotation and the Fold Change represents the expression change relative to the iLuc (control) group.

'

#	GO term	Description	A	B	odds ratio	p-value
1	GO:0006260	DNA REPLICATION	10 (354)	45 (11495)	7,22	0,00037
2	GO:0043138	3'-5' DNA HELICASE ACTIVITY	5 (354)	11 (11495)	14,76	0,00485
3	GO:0055114	OXIDATION-REDUCTION PROCESS	23 (354)	396 (11495)	1,89	0,03
4	GO:0005792	MICROSOME	9 (354)	84 (11495)	3,48	0,05
5	GO:0004364	GLUTATHIONE TRANSFERASE ACTIVITY	6 (354)	37 (11495)	5,27	0,05
6	GO:0004497	MONOOXYGENASE ACTIVITY	8 (354)	87 (11495)	2,99	0,19
7	GO:0005739	MITOCHONDRION	13 (354)	228 (11495)	1,85	0,29
8	GO:0006508	PROTEOLYSIS	23 (354)	532 (11495)	1,40	0,3
9	GO:0030170	PYRIDOXAL PHOSPHATE BINDING	5 (354)	39 (11495)	4,16	0,33
10	GO:0005759	MITOCHONDRIAL MATRIX	6 (354)	56 (11495)	3,48	0,36
11	GO:0008152	METABOLIC PROCESS	13 (354)	238 (11495)	1,77	0,37
12	GO:0004252	SERINE-TYPE ENDOPEPTIDASE ACTIVITY	14 (354)	274 (11495)	1,66	0,42
13	GO:0020037	HEME BINDING	9 (354)	138 (11495)	2,12	0,45
14	GO:0022857	TRANSMEMBRANE TRANSPORTER ACTIVITY	5 (354)	45 (11495)	3,61	0,47

Table 3.1. Gene-Ontology (GO) Terms from up-regulated genes in the iβFTZ-F1 RNA-seq dataset. Genes with a f.c. > 1.3 were selected for GO analysis using R-Spider. Column A depicts the number of genes out of the 354 selected genes to be annotated as the GO-Term. Column B is total number of genes within the *Ae. aegypti* transcriptome to be annotated as the represented GO-Term.

#	GO term	Description	A	B	odds ratio	p-value
1	GO:0055085	TRANSMEMBRANE TRANSPORT	22 (250)	341 (11471)	2,96	0,0024
2	GO:0004252	SERINE-TYPE ENDOPEPTIDASE ACTIVITY	17 (250)	274 (11471)	2,85	0,01
3	GO:0009055	ELECTRON CARRIER ACTIVITY	10 (250)	144 (11471)	3,19	0,01
4	GO:0016021	INTEGRAL TO MEMBRANE	28 (250)	783 (11471)	1,64	0,03
5	GO:0006508	PROTEOLYSIS	22 (250)	532 (11471)	1,90	0,04
6	GO:0005576	EXTRACELLULAR REGION	16 (250)	356 (11471)	2,06	0,05
7	GO:0030170	PYRIDOXAL PHOSPHATE BINDING	5 (250)	39 (11471)	5,88	0,07
8	GO:0006911	PHAGOCYTOSIS, ENGULFMENT	10 (250)	189 (11471)	2,43	0,14
9	GO:0005739	MITOCHONDRION	11 (250)	228 (11471)	2,21	0,17
10	GO:0005811	LIPID PARTICLE	10 (250)	244 (11471)	1,88	0,45

Table 3.2. Gene-Ontology (GO) Terms from up-regulated genes in the iβFTZ-F1 RNA-seq dataset. Genes with a f.c. > 0.7 were selected for GO analysis using R-Spider. Column A depicts the number of genes out of the 250 selected genes to be annotated as the GO-Term. Column B is total number of genes within the *Ae. aegypti* transcriptome to be annotated as the represented GO-Term.

#	GO term	Description	A	B	odds ratio	p-value
1	GO:0006508	PROTEOLYSIS	24 (309)	532 (11497)	1,68	0,08
2	GO:0004252	SERINE-TYPE ENDOPEPTIDASE ACTIVITY	15 (309)	274 (11497)	2,04	0,11
3	GO:0005886	PLASMA MEMBRANE	16 (309)	359 (11497)	1,66	0,26
4	GO:0007498	MESODERM DEVELOPMENT	6 (309)	69 (11497)	3,24	0,35
5	GO:0005576	EXTRACELLULAR REGION	15 (309)	356 (11497)	1,57	0,37
6	GO:0004222	METALLOENDOPEPTIDASE ACTIVITY	6 (309)	78 (11497)	2,86	0,49

Table 4.1. Gene-Ontology (GO) Terms from up-regulated genes in the iE75 RNA-seq dataset. Genes with a f.c. > 1.3 were selected for GO analysis using R-Spider. Column A depicts the number of genes out of the 309 selected genes to be annotated as the GO-Term. Column B is total number of genes within the Ae. aegypti transcriptome to be annotated as the represented GO-Term.

#	GO term	Description	A	B	odds ratio	p-value
1	GO:0005576	EXTRACELLULAR REGION	14 (178)	356 (11465)	2,53	0,02
2	GO:0005811	LIPID PARTICLE	10 (178)	244 (11465)	2,64	0,08

Table 4.2. Gene-Ontology (GO) Terms from down-regulated genes in the iE75 RNA-seq dataset. Genes with a f.c. > 0.7 were selected for GO analysis using R-Spider. Column A depicts the number of genes out of the 178 selected genes to be annotated as the GO-Term. Column B is total number of genes within the Ae. aegypti transcriptome to be annotated as the represented GO-Term.

CHAPTER IV

Function role of juvenile hormone controlled miRNAs in mosquito reproductive physiology

4. 1 Abstract

MicroRNAs play a critical role in regulating genes and pathways essential for different physiological processes during the gonotrophic cycle. We have demonstrated that the transcription factor E75 is critical for regulating miRNA expression in the fat body tissue during the post-eclosion (PE) developmental phase. Here, we examine the role E75 regulated miRNAs, *miRNA-276*, *miRNA-2940* and *miR-252*, play during the gonotrophic cycle. For this analysis, we first performed antagomir knockdowns to functionally block miRNA activity, and subsequently measured the primary follicle development and the number of eggs laid by female individuals. Of the three antagomirs investigated, only treatment with Ant-2940-3p resulted in reduced follicle size and number of eggs laid. Next, we performed computational mRNA-miRNA target predictions to elucidate the mRNA gene(s) affected by *miR-2940* knockdown. From the potential list of predicted mRNA gene targets, *AAEL002518* was the only transcript to have elevated gene levels, which we confirmed by RT-qPCR *in vivo* from *Ant-2940-3p* treated fat body tissues. We identified *AAEL002518* as the potential target of *miRNA-2940-3p* and confirmed the mRNA-miRNA interaction using an *in vitro* dual luciferase assay in *Drosophila* S2 and in native *Ae. aegypti* Aag2 cell lines. Finally, we performed a phenotypic rescue experiment to demonstrate that elevated expression of *AAEL002518* was responsible for the disruption noted in egg

development. Collectively, these results indicate the importance of *miR-2940-3p* in the fat body tissue during the PE developmental phase of the gonotrophic cycle.

4.2 Introduction

MicroRNAs (miRNA) play a critical role in regulating gene expression during the gonotrophic cycle of *Aedes aegypti.* Prior studies have demonstrated that miRNAs have a significant impact on regulating different mosquito biological processes. *MiR-275* was shown to target *sarco/endoplasmic reticulum* Ca^{+2} *adenosine triphosphates* (*SERCA*) to control proper blood digestion in the midgut and *miR-8* regulates the Wingless signaling pathway in the fat body for secretion of lipids into the hemolymph during vitellogenesis[1-3]. Inhibition of both of these miRNAs results in biological defects that lead to egg inhibition and prevents mosquito reproduction. Expression of both of these miRNAs were also spatially validated through the use of tissue specific transgenic-sponges.

Newer advancements in genome-editing tools using CRISPR/Cas9 have allowed for the generation of miRNA-specific mutations in mosquitoes that have had a more profound impact of reproductive physiology. Embryonic injection of Cas9 protein and a sgRNA designed against *miR-309, the* target of Homeobox gene *SIX4*, and *miR-277*, target of *insulin-like peptide-7* and *insulin-like peptide-8*, completely inhibited egg development[4,5]. Individual mosquitoes were screened and confirmed by Sanger sequencing to have highly-polymorphic mutations in the sgRNA targeted region, demonstrating the successful genomic disruption by Cas9. Here, we explore the functional role of E75 regulated miRNAs, *miR-276*, *miR-2940* and *miR-252* during the PE developmental phase.

We defined the impact of *miRNAs* on primary follicle development and egg production during the gonotrophic cycle and found only *miR-2940-3* to negatively regulate reproductive physiology. We used *in silico* target predictions and *in vitro* luciferase based cell culture experiments and identified that *miR-2940-3p* action is mediated through the regulation of the glutamate receptor, *clumsy*. Performing a phenotypic rescue experiment, we confirm that over-expression of *clumsy* results in disruption in reproduction. Overall, these results demonstrate a novel role for *miRNA-2940-3p* during the PE developmental phase in the fat body tissue required for proper reproductive functions.

4.3 Methods

Double-stranded RNAi injections

DsRNAs for *iLuc*, and *iAAEL002518* were synthesized using the MEGAscript Kit (Ambion). Synthetic antagomirs were obtained from Dharamcom using the custom single strand RNA synthesis protocol. At 12 hr PE, 0.5μg (.25μl of 2μg/μl) dsRNA or 50pmol (200μM/.25μl) antagomir was injected into the thorax of adult female mosquitoes. Mosquitoes were allowed to recover for 3-4 days on both H_20 and sugar water before dissection and fat body tissue collection. For rescue experiments, mosquitoes were co-injected with a mixture of dsRNA/antagomir at a final concentration of 2μg/μl and 200μM antagomir, respectively.

Reverse Transcriptase Quantitative PCR

Total RNA was prepared using Trizol (Invitrogen) following the standard protocol. Total RNA was purified using Zymo RNA cleanup kit (R1018) and in-column DNase treatment (E1010). Total RNA was quantified using Nanodrop 2000 and 2.5µg was subjected to cDNA synthesis using the SuperScript III Kit (Invitrogen). Expression data was plotted as $2^{-\Delta Ct}$ whereby the cycle threshold (Ct) for the gene of interest is compared with the Ct of the internal control gene. All expression data are plotted as relative expression to *actin*.

MiRNA Computational Target Predictions:

The 3'UTRs were extracted from the AaegL5.1 genome database. UTRs were specifically selected from genes that displayed a > 1.3 Log2 fold change from the iE75 dataset. The miRNA-mRNA target prediction programs miRanda and RNAhybrid were then used for best match with the mature aae-miR-2940-3p sequence.

Chemical Injections

AP-5 (A5282), Kainic acid (K02050), AMPA (A6816) and L-Glutamic acid (G8415) were purchased from Sigma-Millpore. Solutions were dissolved in H_20 and following stock solutions were utilized for injections: AP-5 (100nM), Kainic Acid (1M), AMPA (5mM) and Glutamic Acid (1mM). Female mosquitoes injected with .25µl of each individual solution. For the AP-5 rescue experiment, mosquitoes were co-injected with a mixture of AP-5/antagomir at a final concentration of 50 nM AP-5 and 200µM antagomir,

respectively. Mosquitoes were allowed to recover for 3-4 days on both H_20 and sugar water before blood feeding.

Cell Culture and Luciferase Assay

PCR products containing full-length *AAEL002518* 3′ UTR (based on AaegL5.1 annotations) were prepared from FB-specific cDNA templates. The 3′ UTR were amplified with primers containing *Not*I or *Eco*RV sites and cloned downstream of *Renilla luciferase* in psiCheck-2 vector (Promega). For mutagenesis of site-1 and site-2, 7mer miRNA seed complements in the predicted miR-2940-3p binding sites were mutated using Q5 Site-Directed Mutagenesis kit (NEB). For *Drosophila* S2 cell transfection, 100ng of psiCheck-2 reporters and either synthetic aae-mir-2940-3p miRNA mimic (Qiagen) or Allstars Negative control siRNA (Qiagen) at a final concentration of 100nm were co-transfected using Attractene Transfection reagent (Qiagen). For *Ae. aegypti* Aag2 cell, 100ng of psiCheck-2 reporters were transfected using Fugene HD (Promega). The dual luciferase assay was completed 24 hr post-transfection using the Dual Luciferase Reporter Assay System (Promega). Firefly luciferase levels were used for normalization of Renilla luciferase expression level. Treatments were performed in triplicates, and transfections were repeated three times.

4.4 Results

We set out to examine the functional roles of *miR-2940-3p*, *miR-276-3p* and *miR-252-5p* during the gonotrophic cycle. Synthetic RNA probes complementary to the mature

miRNA strand, termed antagomirs, were designed and injected into adult female mosquitoes 6-24 hr PE. Four days post injection, female mosquitoes were provided a blood meal and subsequently examined for primary follicle development 24 hr post feeding. We found that treatment with Ant-2940-3p impaired priimary follicle development growth, average length of 182 µM, in comparison to the wild-type and antagomir control groups, average length of 220 µM and 221 µM, respectively (Figure 1A). Concordantly, we measured egg laying numbers and found that Ant-2940-3p females had fewer eggs deposited, average number of 57 eggs per female, in comparison to the wild-type and antagomir control groups, both of which had an average of 90 eggs per female (Figure 1B). Treatment with either Ant-276-3p or Ant-252-5p had no major impact on the reproductive cycle when similarly analyzed. These experiments highlight the importance of *miR-2940-3p* in egg production during the gonotrophic cycle.

To identify the molecular target of *miR-2940-3p*, we utilized an *in silico* approach using different bioinformatic miRNA target prediction programs. Our previous results indicated that *miR-2940-3p* is regulated through the transcription factor E75. Thus, we specifically selected the 3'UTRs from the genes whose expressions were up-regulated in the iE75 RNA-seq results as the reference dataset for miRNA target investigation. The predicted mRNA-miRNA interactions using the two bioinformatic programs, miRanda and RNA hybrid[6], produced nine genes as having a *miR-2940-3p* binding site (Table 1). To confirm an authentic mRNA target, we screened for elevated gene expression levels *in vivo* by RT-qPCR from fat body tissue treated with Ant-2940-3p. Out of the nine predicted mRNA target list, only *AAEL002518* demonstrated to have an increased gene expression

level in comparison to the WT and Ant-Scr groups, respectively (Figure 2.1). The UniProt database defines *AAEL002518* as glutamate ion channel, containing both a transmembrane domain and ligand-binding site for glutamate or glycine. A protein BLAST search suggests that *AAEL002518* is homologous to the *Drosophila* gene *clumsy*. These data suggest that *AAEL002518* is either directly or indirectly regulated through the actions of *miRNA-2940-3p.*

To assess whether *AAEL002518* is the authentic target of *miR-2940-3p*, we utilized a cell culture based luciferase assay. The 3'UTR of *AAEL002518* was cloned downstream of the *Renilla* translational stop codon within the psiCheck-2 vector to generate a 3'UTR-fused luciferase reporter. The reporter vector was then transfected into *Drosophila* S2 cells along with a *miR-2940-3p* mimic and luciferase activity was measured 24 hr post transfection. We found that the addition of the *miR-2940-3p* mimic resulted in a 20% reduction in luciferase activity in comparison to the treatment group containing the Allstar mimic (negative siRNA control) (Figure 3.1). Our bioinformatic predictions identified two potential binding sites *for miR-2940-3p* within the 3'UTR of *AAEL002518*, we refer to as Site-1 and Site-2. To identify the specific-site that *miR-2940-3p* binds on the UTR transcript, we performed a site-directed mutagenesis assay to scramble the seed sequence to abolish the miRNA-mRNA interaction and alleviate luciferase repression. The mutation in Site-1 alleviated the repressive effect by *miR-2940-3p* mimic, while the mutation in Site-2 still resulted in a ~20% reduction in luciferase activity in comparison to the Allstar control group (Figure 3.2). This result confirms that miR-2940-3p mediated repression of *AAEL002518* is directed through Site-1 on the 3'UTR.

As *miR-2940-3p* is a Culicinae subfamily specific miRNA, we additionally performed the transfection experiments in the native *Ae. aegypti* Aag2 cell line using the endogenous miRNA as a substitute for the miRNA mimic. Transfection of Aag2 cells with psiCheck-2 vector containing the 3'UTR resulted in a ~15% decrease of luciferase activity in comparison to the empty psiCheck-2 vector. Mutating Site-1 restored luciferase levels to the empty psiCheck-2 vector, while mutating Site-2 still resulted in luciferase reduction (Figure 3.3). This finding further supports our results obtained using the S2 cell line where Site-1 was found to be responsible for mediating transcript repression. The combination of both the *in vitro* S2 and Aag2 cell based results further strengthen our findings that *AAEL002518* is an authentic target of *miR-2940-3p*.

We next confirmed that upregulation of *AAEL002518* is responsible for the reproductive defects we noted in the *Ant-2940-3p* treatment experiments. We performed a phenotypic rescue experiment by simultaneous knockdown of *miR-2940-3p* and *AAEL002518* in the same individuals. We synthesized dsRNA targeting *AAEL002518* and mixed it with synthetic *Ant-2940-3p*, using a final concentration of 2 µg/µl and 200 µmol/µl, respectively. Depleting *AAEL002518* along with *Ant-2940-3p* treatment partially restored primarily follicle development, average length of 193 µM, in mosquitoes to the level noted in the Ant-Scr/iLuc and WT groups, average length of 205 µM and 213 µM respectively, confirming that up-regulation of *AAEL002518* is responsible for the reproductive defects caused by *Ant-2940-3p* treatment (Figure 4.1). We additionally measured number of eggs laid and coordinately found *clumsy* RNAi, 69 eggs per female,

to restore egg deposition in comparison to the Ant-2940-3p treatment, 59 eggs per female (Figure 4.2).

AAEL002518 is the *Drosophila* homolog of *clumsy*, an ionotropic glutamate receptor belonging to the subtype kainate receptors. Glutamate receptors contain a ligand binding-domain, responsible for binding the amino acid glutamate and a transmembrane channel for trafficking different ions across the cell membrane. To mimic the genetic overexpression response by Ant-2940-3p, groups of mosquitoes were treated by injection with either 100 mM of glutamate and 10 mM of kainic acid, an agonist specific for the kainate receptor subgroup or H_20 as control respectively (Figure 5.1). Both treatment groups showed no impact on primary follicle development relative to the control suggestive that the treatments were not capable of inducing Clumsy activity. It is possible that Clumsy has a weak binding affinity towards the tested compounds and thus is incapable of inducing a response to the given treatment. We attempted to mimic our phenotypic rescue experiments using AP-5, a synthetic antagonist of kainate receptors, as a substitute for dsRNA targeting *AAEL002518*. The mixture of Ant-2940-3p and AP-5 was able to rescue both primary follicle growth, average length of 209 µM, and egg development suggestive that Clumsy was effectively inhibited via chemical treatment (Figure 4.1 and Figure 4.2). These experiments demonstrate that the up-regulation of Clumsy is responsible for the reproductive defect noted by Ant-2940-3p treatment.

4.5 Discussion

Here we set out to identify the functional role(s) of the E75-regulated miRNAs, *miR-2940-3p, miR-276-3p* and *miR-252-5p* during the gonotrophic cycle. Using synthetic antagomirs to block mature miRNA function, we were able to identify *miR-2940-3p* as a candidate for egg production. Inhibition of *miR-2940-3p* impaired both primary follicle development and overall female egg laying numbers, suggestive that this miRNA has regulatory function in the gonotropic cycle. Although *miR-276-3p* and *miR-252-5p* were also shown to be regulated by E75, their inhibition had no effects on egg development and it is likely that their functions may be tied to another aspect of mosquito physiology different from the reproductive cycle.

The *miR-2940* locus is specific to Culicinae subfamily, present in *Culex, Anopheles* and *Aedes* mosquitoes, while being absent in other Dipteran species, such as *Drosophila* and *Glossina* flies. The *miR-2940* locus was originally identified through small RNA-sequencing analysis from *Ae. albopictus* C7/10 cell line and displayed the -5p arm as the predominate strand[7]. Further research has mostly centered on the -5p arm showing its functional importance in *Wolbachia* endosymbiont colonization success and immune effects aiding in vector resistance to viral infections of Dengue and West Nile Virus[8-10]. Hence, functions of *miR-2940-3p* were previously largely unexplored in the mosquito biology. Our prior and current small RNA sequencing datasets from the female adult fat body indicate that the -3p arm is the predominately expressed miRNA. This finding is also corroborated with tissue-specific sequencing results from *A. gambie,* indicating that perhaps a miRNA arm switching event occurs at some point in the mosquito life cycle.

The molecular target for *miR-2940-3p* was previously unknown. Our small RNA sequencing dataset from E75 knockdown fat body tissue displayed a reduction in *miR-2940-3p* expression, and thus we reasoned this would also be reflected by an increase of mRNA transcripts regulated by miR-*2940-3p*. We specifically curated the 3'UTR sequences from mRNA transcripts upregulated in the iE75 RNA-seq analysis for potential *miR-2940-3p* interactions. Using the consensus mRNA targets predicted by two independent bioinformatic programs, miRanda and RNAhybrid, we obtained nine potential transcripts displaying a miRNA-mRNA interaction with *miR-2940-3p*. RT-qPCR analysis from Ant-2940-3p treated fat body samples implicated *AAEL002518* as the bonified direct or indirect target of *miR-2940-3p* as only this gene showed significantly elevated levels of expression. We utilized an *in vitro* luciferase based assay in both *Drosophila* S2 and the native *Ae. aegypti* Aag2 cell culture lines to verify the activity and specific binding site of *miR-2940-3p* on the 3'UTR of *AAEL002518*. These *in vitro* results confirm our *in vivo* findings that *miR-2940-3p* regulates *AAEL002518* expression in the fat body tissue during the PE phase.

To address whether the inhibition of primary follicle and egg development was a direct result of *AAEL002518* overexpression, we performed a phenotypic rescue experiment to silence *miR-2940-3p* and *AAEL002518* simultaneously in individual mosquitoes. Inhibiting both *miR-2940-3p* and *AAEL002518* restored the primary follicle length and egg laying numbers, indicating that upregulation of *AAEL002518* levels is responsible for the reproductive defects noted by silencing of *miR-2940-3p* via the Ant-2940-3p treatment. In *Drosophila, AAEL002518* encodes the protein Clumsy, which is an

ionotropic glutamate receptor, belonging to the subtype kainate receptors[11]. Based on research performed in the vertebrate system, there are three subtypes of ionotropic glutamate receptors; kainate, AMPA and NMDA, termed for their ability to be activated by that specific pharmacology-based compound[12]. All three glutamate receptor subtypes are principally involved in neurophysiology and regulate trafficking of Na^{2+}, K^{+}, Ca^{2+} across the cell membrane to initiate a specific downstream cellular process. Although their annotations are based on homology with the vertebrate systems, the functional properties and activity against the predicted pharmaceutical compound may differ between vertebrate and insect system. For example, the kainate receptor DkaiR1D can be inhibited by a NMDA-specific compound AP-5 and AMPA receptor DGluR1A can be activated by kainic acid rather than the predicted AMPA compound[13]. This finding further supports our observations that while *clumsy* is identified as homologous to a vertebrate kainate receptor, Clumsy from the vertebrate and invertebrate systems may differ and that treatment with kainic acid is unable to block this receptor's functions, similar to what we noted upon antagomir treatment.

4.6 References

1 Bryant, B., Macdonald, W. & Raikhel, A. S. microRNA miR-275 is indispensable for blood digestion and egg development in the mosquito Aedes aegypti. *Proc Natl Acad Sci U S A* **107**, 22391-22398, doi:10.1073/pnas.1016230107 (2010).

2 Zhao, B. *et al.* MicroRNA-275 targets sarco/endoplasmic reticulum Ca2+ adenosine triphosphatase (SERCA) to control key functions in the mosquito gut. *PLoS Genet* **13**, e1006943, doi:10.1371/journal.pgen.1006943 (2017).

3 Lucas, K. J. *et al.* MicroRNA-8 targets the Wingless signaling pathway in the female mosquito fat body to regulate reproductive processes. *Proc Natl Acad Sci U S A* **112**, 1440-1445, doi:10.1073/pnas.1424408112 (2015).

4 Ling, L., Kokoza, V. A., Zhang, C., Aksoy, E. & Raikhel, A. S. MicroRNA-277 targets insulin-like peptides 7 and 8 to control lipid metabolism and reproduction in Aedes aegypti mosquitoes. *Proc Natl Acad Sci U S A* **114**, E8017-E8024, doi:10.1073/pnas.1710970114 (2017).

5 Zhang, Y. *et al.* microRNA-309 targets the Homeobox gene SIX4 and controls ovarian development in the mosquito Aedes aegypti. *Proc Natl Acad Sci U S A* **113**, E4828-4836, doi:10.1073/pnas.1609792113 (2016).

6 Kruger, J. & Rehmsmeier, M. RNAhybrid: microRNA target prediction easy, fast and flexible. *Nucleic Acids Res* **34**, W451-454, doi:10.1093/nar/gkl243 (2006).

7 Skalsky, R. L., Vanlandingham, D. L., Scholle, F., Higgs, S. & Cullen, B. R. Identification of microRNAs expressed in two mosquito vectors, Aedes albopictus and Culex quinquefasciatus. *BMC Genomics* **11**, 119, doi:10.1186/1471-2164-11-119 (2010).

8 Hussain, M., Frentiu, F. D., Moreira, L. A., O'Neill, S. L. & Asgari, S. Wolbachia uses host microRNAs to manipulate host gene expression and facilitate colonization of the dengue vector Aedes aegypti. *Proc Natl Acad Sci U S A* **108**, 9250-9255, doi:10.1073/pnas.1105469108 (2011).

9 Zhang, G., Hussain, M., O'Neill, S. L. & Asgari, S. Wolbachia uses a host microRNA to regulate transcripts of a methyltransferase, contributing to dengue virus inhibition in Aedes aegypti. *Proc Natl Acad Sci U S A* **110**, 10276-10281, doi:10.1073/pnas.1303603110 (2013).

10 Slonchak, A., Hussain, M., Torres, S., Asgari, S. & Khromykh, A. A. Expression of mosquito microRNA Aae-miR-2940-5p is downregulated in response to West Nile virus infection to restrict viral replication. *J Virol* **88**, 8457-8467, doi:10.1128/JVI.00317-14 (2014).

11 Littleton, J. T. & Ganetzky, B. Ion channels and synaptic organization: analysis of the Drosophila genome. *Neuron* **26**, 35-43, doi:10.1016/s0896-6273(00)81135-6 (2000).

12 Traynelis, S. F. *et al.* Glutamate receptor ion channels: structure, regulation, and function. *Pharmacol Rev* **62**, 405-496, doi:10.1124/pr.109.002451 (2010).

13 Li, Y. *et al.* Novel Functional Properties of Drosophila CNS Glutamate Receptors. *Neuron* **92**, 1036-1048, doi:10.1016/j.neuron.2016.10.058 (2016).

4.7 Figures and Tables

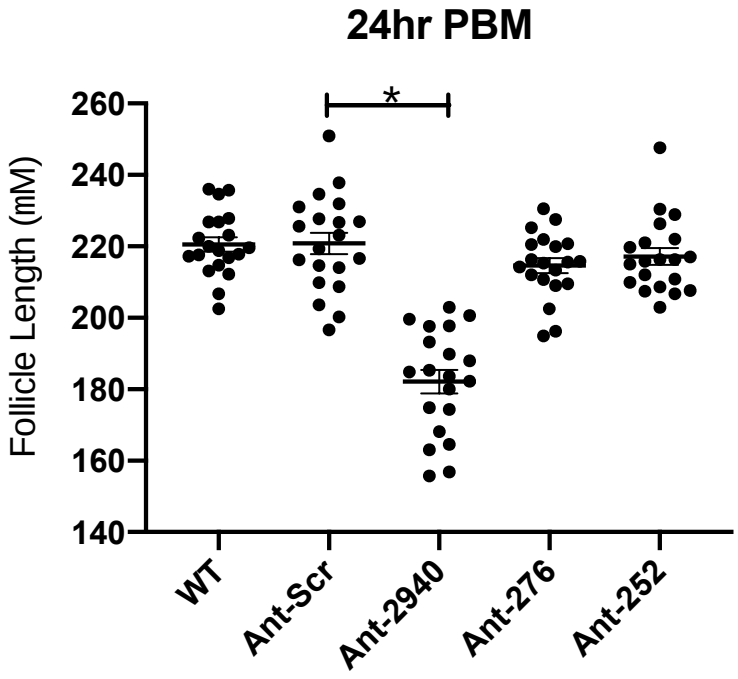

Figure 1.1: Average follicle size measured from Wild-Type (WT) Ant-Scr, Ant-2940, Ant-276 and Ant-252 treated mosquitoes at 24 hours PBM. Each data point represents one biological individual derived from five different technical measurements. Each individual experiment consists of five biological points per group, with experiments being repeated independently four times. $*P < 0.05$, Statistical significance was calculated using an unpaired Student's T-test.

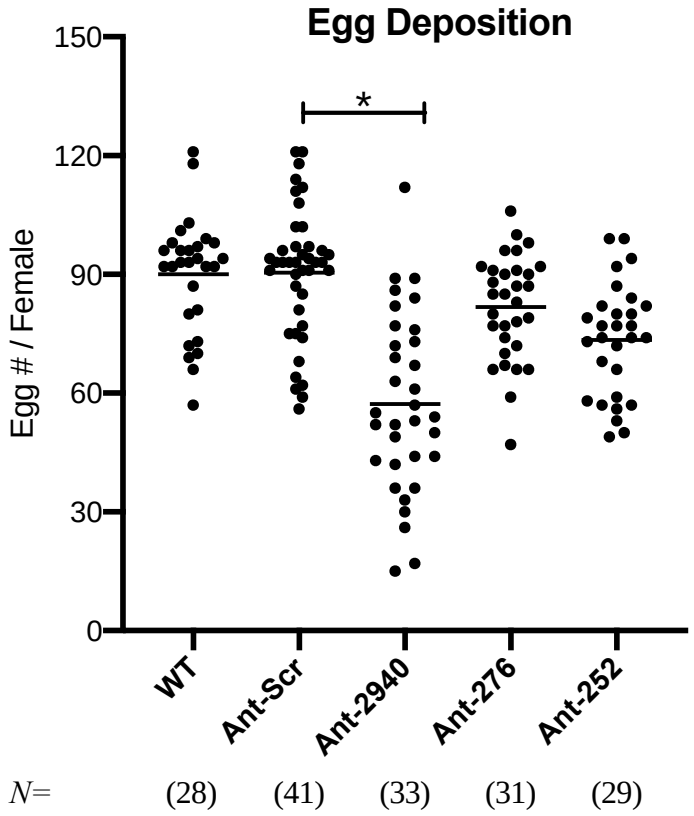

Figure 1.2: Number of eggs laid per female mosquito from Wild-Type (WT), Ant-Scr, Ant-2940, Ant-276 and Ant-252 individuals. Each data point represents the number of eggs laid by an individual female. *$P < 0.05$, Statistical significance was calculated using unpaired Student's T-test.

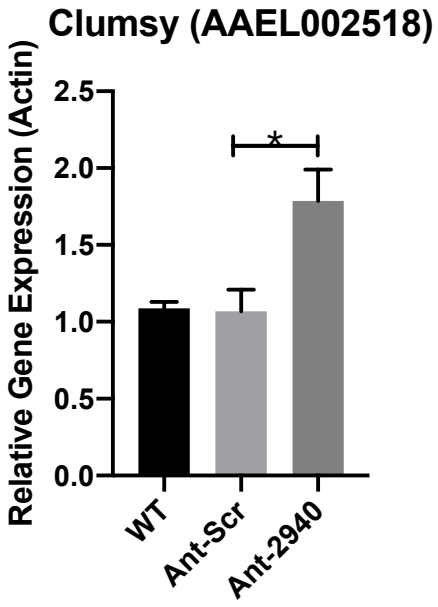

Figure 2.1: Relative gene expression level for clumsy (AAEL002518) measured by qPCR from fat body tissue in WT, Ant-Scr and Ant-2940 treated individuals. Each experiment consisted of 3-4 biological samples and each experiment was repeated a total of three independent times. Statistical significance was calculated using a one-way ANOVA. *$P <$ 0.05, Relative expression levels are represented mean ± SEM.

(a)

```
dataset: 1
target: AAEL002518
length: 697
miRNA : aae-miR-2940-3p
length: 22

mfe: -15.5 kcal/mol
p-value: 1.000000e+00

position  58
target 5'  U        G AG       A 3'
            UGA   AU U  UUGUCGA
            ACU   UA A  GACAGCU
miRNA  3' UC   AAA  G GG       G 5'
```

(b)

```
dataset: 1
target: AAEL002518
length: 697
miRNA : aae-miR-2940-3p
length: 22

mfe: -16.7 kcal/mol
p-value: 1.000000e+00

position  353
target 5'    A     G   AAA        U 3'
              AUUUA   C   CUGUUGAU
              UAAAU   G   GACAGCUG
miRNA  3' UCAC     AGA G            5'
```

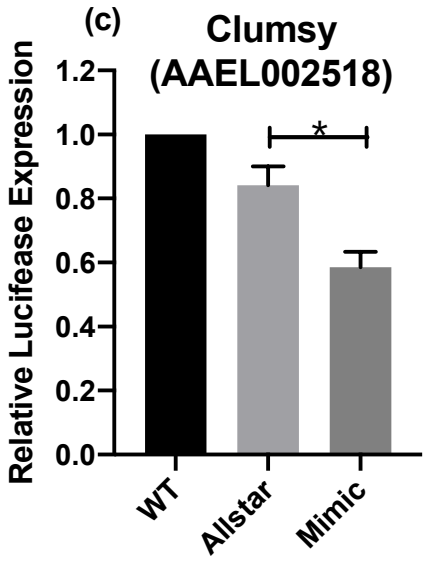

Figure 3.1: miR-2940-3p targets the 3'UTR of Clumsy (AAEL002518). (a) and (b), Putative miR-2940-3p target predictions on the 3'UTR of Clumsy from *in silico* analysis using miRanda. (C) Dual luciferase reporter assay for Clumsy (AAEL002518) in Drosophila S2 cells. Results are expressed as the relative ratio of Renilla luciferase activity to Firefly luciferase activity. Statistical significance was calculated using an unpaired Student's T-test. *$P < .05$, Data represent three biological replicates with three technical replicates and are shown as average ± SEM.

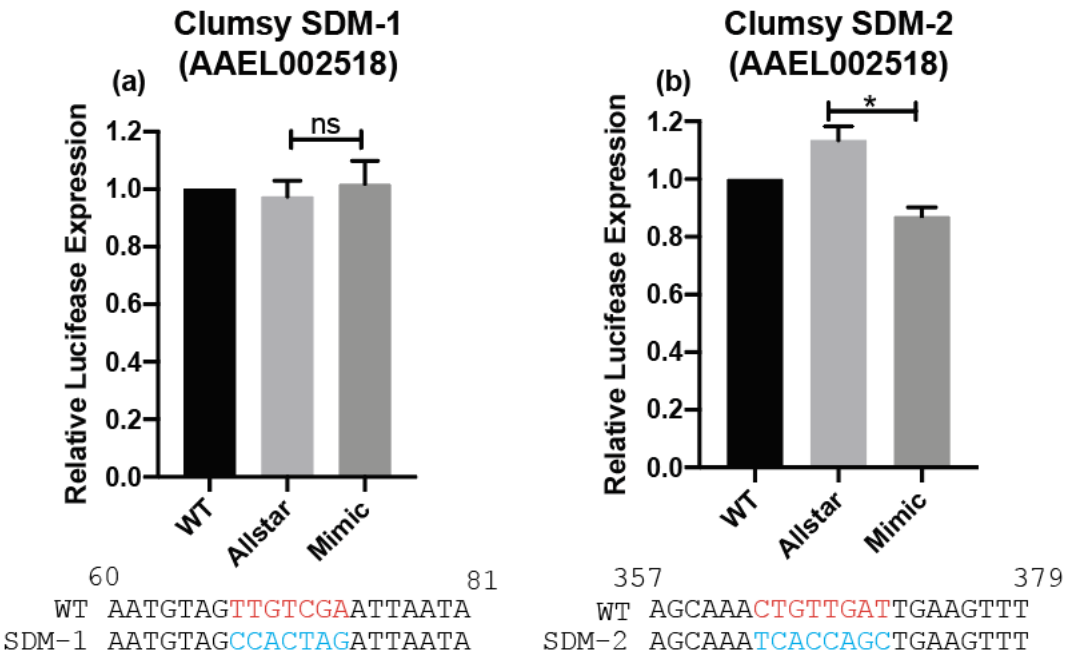

Figure 3.2 Dual luciferase reporter assay for Clumsy (AAEL002518) using mutated plasmids in Drosophila S2 cells. (A) and (B), Independent plasmids were generated with mutations on the 3'UTR in the potential "seed" sequence for the predicted miR-2940-3p binding site. The seed sequences are highlighted in blue and the corresponding substitutions on the mutated plasmid are highlighted in red. Results are expressed as the relative ratio of Renilla luciferase activity to Firefly luciferase activity. Statistical significance was calculated using an unpaired Student's T-test. Data represent three biological replicates with three technical replicates and are shown as average ± SEM.

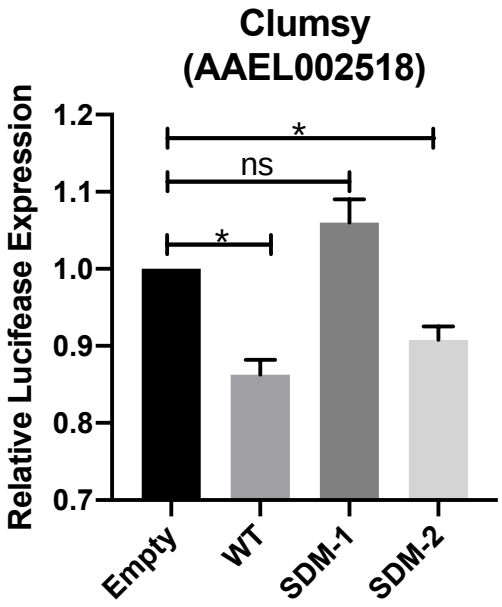

Figure 3.3 Dual luciferase reporter assay for Clumsy (AAEL002518) using *Ae. aegypti* Aag2 cells. Results are expressed as the relative ratio of Renilla luciferase activity to Firefly luciferase activity. Statistical significance was calculated using an unpaired Student's T-test. *$P < .05$, Data represent three biological replicates with three technical replicates and are shown as average ± SEM.

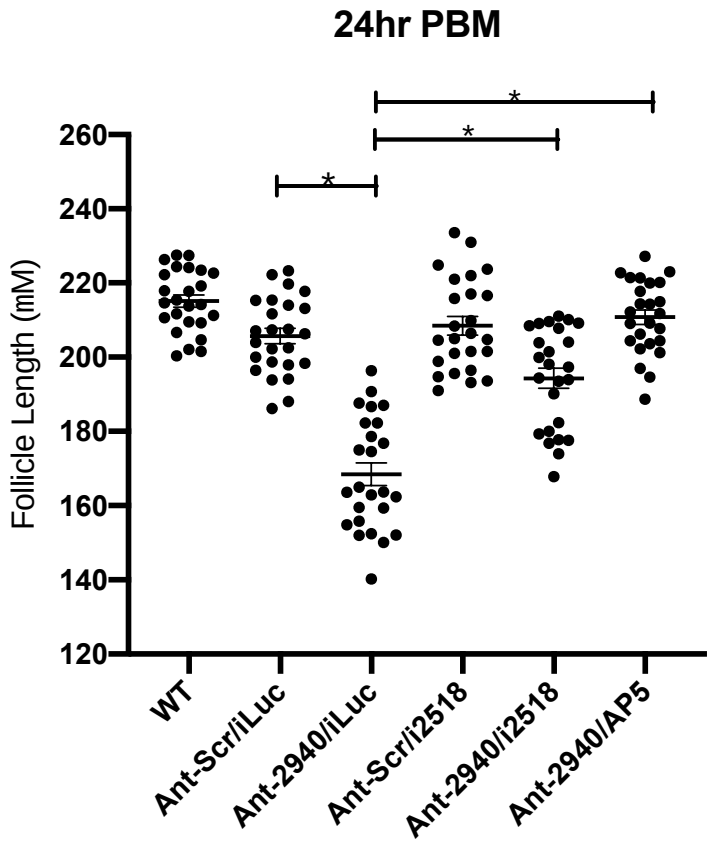

Figure 4.1: Average follicle size of wild-type (WT), Ant-Scr/iLuc, Ant-2940/iLuc, Ant-Scr/i2518, Ant-2940/i2518 and Ant-2940/AP-5 treated mosquitoes at 24 hours PBM. Each data point represents one biological individual derived from five different technical measurements. Each individual experiment consists of five biological points per group, with experiments being repeated independently four times. *$P < .05$, Statistical significance was calculated using an unpaired Student's T-test.

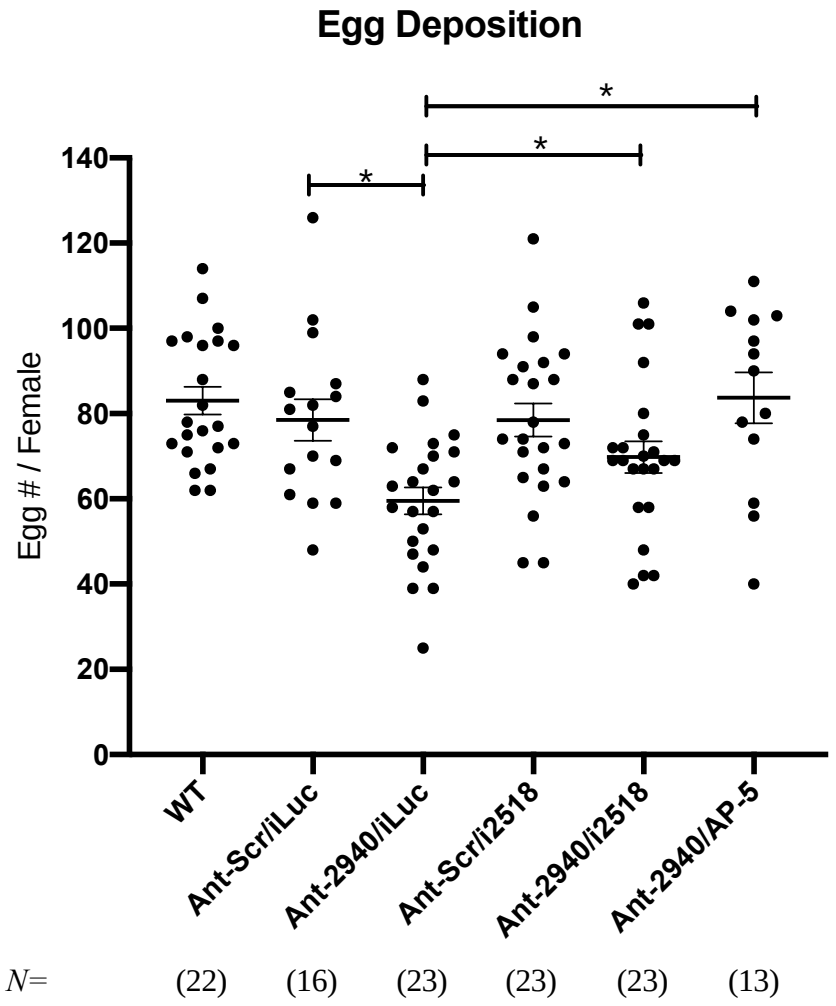

Figure 4.2: Number of eggs laid per female mosquito wild-type (WT), Ant-Scr/iLuc, Ant-2940/iLuc, Ant-Scr/i2518, Ant-2940/i2518 and treated mosquitoes. Each data point represents the number of eggs laid by an individual female. Statistical significance was calculated using unpaired Student's T-test. *$P < .05$.

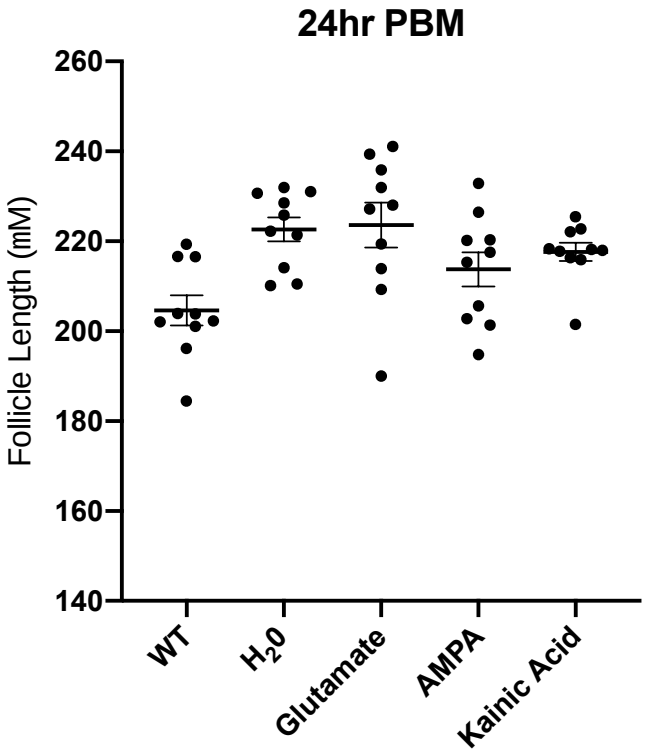

Figure 5.1: Average follicle size of wild-type (WT), H_20, Glutamate, AMPA and Kainic Acid treated mosquitoes at 24 hours PBM. Each data point represents one biological individual derived from five different technical measurements. Each individual experiment consists of five biological points per group, with experiments being repeated independently two times.

Genes IDs	Annotations
AAEL013462	jbug
AAEL025524	Xpd
AAEL000860	uzip
AAEL022689	Usp10
AAEL027536	CD98hc
AAEL002518	clumsy
AAEL005206	Mur89F
AAEL004392	IMP
AAEL001119	E(bx)

Table 1.1 Shared genes predicted by *in silicio* analysis from miRanda and RNAhybrid to have a potential *miR-2940-3p* binding site within the 3'UTR.

CHAPTER V

Conclusion of the Dissertation

5.1 Discussion

MiRNAs play a critical role in regulating multiple physiological processes, including reproduction in the disease vector *Ae. aegypti*. Our presented research demonstrates a novel approach to identifying critical miRNA-mRNA interactions by deciphering the transcriptional factors that mediate miRNA expression. The initial findings aimed at identifying novel pri-miRNAs in the *Ae. aegpyti* genome through RNA-seq analysis from Drosha knockdown individuals. From our analysis, we were able to identify two novel pri-miRNAs for *miRNA-252* and *miRNA-2940,* and confirm a previously annotated pri-miRNA for *miR-276*. Although our approach was capable of identifying novel transcripts, the majority of miRNAs in the *Ae. aegpyti* genome are still unannotated, suggesting that an additional methodology is required to further expand the reference database. The use of a ribosomal depletion kit could aid in identifying pri-miRNAs that may not be poly-A adenylated as previously described in the vertebrate system.

Next, we set out to identify the transcriptional regulators of the novel pri-miRNAs. Previously completed *in vitro* and *in vivo* studies with the *Drosophila* model system established the role of specific hormonally regulated transcription factors as key candidates governing miRNA expression. We utilized an *in vitro* luciferase based experimental design in *Drosophila S2* cells in which different juvenile hormone controlled transcription factors were additionally expressed along side the candidate pri-miRNAs. Using this transcription factor screen, we noted an increase of luciferase expression only with the addition of E75.

We next identified the specific region E75 bound on the promoter sequence by utilizing a "promoter bashing" strategy. We were able to identify the E75-binding DNA region upstream of the *pri-miR-2940* promoter and then confirmed the DNA base pairs required for the binding through a mutagenesis assay. These *in vitro* experiments highlighted and confirmed the novel role for E75 as a transcriptional regulator of miRNAs in *Ae. aegypti*.

E75 has been largely connected to the ecdysone signaling pathway. We performed a series of experiments *in vivo* to evaluate E75's potential in the juvenile hormone hierarchical network. We took two different approaches to dissect the involvement of JH in E75 regulation. First, we applied JH topically to artificially induce a JH response and next we performed dsRNA treatment of the Met receptor to artificially block the JH pathway and measured E75 gene expression levels from both treatments. Both experiments demonstrated that the E75 transcriptional profile matches the previously identified JH transcription factors for Kr-H1 and Hairy. Our previously completed analysis using mRNA sequencing for both Hairy and Kr-H1 found a high overlap of similarly regulated transcripts between the individual factors and Met. This high transcriptional overlap suggests that both Hairy and Kr-H1 function downstream of Met in the JH hierarchical network. Next, we performed small RNA sequencing experiments from both iMet and iE75 fat body tissues to understand the global profiles changes in small RNA expression. Using the same conceptual strategy as described above, we found a high overlap of the up and down regulated transcripts between the iE75 and iMet treatment groups. Interestingly, we found that the majority of miRNAs were down-regulated in both the iMet and iE75 groups, with iE75 having a larger impact on miRNA expression. This finding supports our

previously described luciferase experiments that demonstrate E75 as an activator of pri-miRNA expression. We also assessed potential JH regulators of E75 and determined through both mRNA-seq and RT-qPCR analysis that βFTZ-F1 specifically targeted E75 transcription, suggestive of a direct or indirect role in its regulation of E75 during this phase. Collectively, these experiments provide further support for our hypothesis that E75 is part of the JH hierarchical network.

Our final aim for this research project was to connect the functional link between E75 regulated miRNAs and their respective role in reproductive physiology. Using a synthetic antagomir to block miRNA function, we obtained a decrease in primary ovarian follicle size and number of eggs deposited upon inhibition of *miR-2940-3p.* Using the iE75 RNA-seq dataset, we scanned for predicted *miRNA-2940-3p* binding sites on the 3'-UTRs of genes up-regulated upon E75 knockdown. The *in silico* analysis lead to the identification of the glutamate receptor, *clumsy*, as the predicted target for *miR-2940-3p*. We found elevated transcript levels of *clumsy* in Ant-2940-3p treated fat body samples and using an *in vitro* luciferase cell culture based assay we confirmed the direct binding of the miR-2940 to the *clumsy* 3'UTR. Finally, we performed a phenotypic rescue experiment to simultaneously knockdown miR-2940-3p and *clumsy*, which confirmed their interaction and returned the ovarian development and egg production defects back to wild-type levels.

Overall, these experiments not only highlight an unprecedented role for E75 as a factor within the juvenile hierarchical network, but also demonstrate E75 as a critical regulator of miRNA expression in the fat body tissue. Our previous results had only identified Kr-H1 and Hairy as transcriptional repressors during this phase, leaving the role

of transcriptional activators unknown. Here, we discovered that E75 is linked to juvenile hormone regulation and has a role in directly activating miRNA expression. As E75 is a highly conserved protein among Dipteran organisms, this research has to potential to expand our knowledge on hormonal regulation and development in a multitude of other insect systems. Currently, little information is known about the different regulatory factors governing miRNA expression and how that information could be linked to different physiological processes. Using our established findings on E75 regulation of *miR-2940-3p*, we were capable for narrowing down the list of potential mRNA targets in the *Ae. aegypti* transcriptome using a combination of RNAi targeting E75 and high-throughput RNA sequencing. This novel approach to highlight potential miRNA-mRNA interactions has yet to be explored in previously completed research studies. We successfully demonstrate this methodology to identify the miRNA-mRNA interaction for *miR-2940-3p* and *clumsy*. While this approach was successfully applied to reproductive physiology, it can be extended to numerous other research applications in vector biology.

Finally, we investigated the involvement of the glutamate receptor Clumsy in the biological process of reproductive physiology. The underlying molecular mechanism of how the over-activation of Clumsy during the PE developmental phase leads to an inhibition of primary ovarian and egg development still needs to be examined. The down-stream signaling response activated by Clumsy and the impact on fat body development can be critical to designing a novel reproductive control strategy. Although glutamate receptors are highly conserved in eukaryotic systems, the potential ligands have evolutionary differed between vertebrate and insect system. This underlines a prospective

control strategy where a chemical agonist could be used to specifically target *Ae. aegypti* Clumsy and would be ineffective in activating the vertebrate homolog. Future studies need to address the functional properties, both electrophysiological and crystallography, of Clumsy are required to identify a unique compound. Overall, these experiments further our knowledge of *Ae. aegypti* gene regulation and understanding of reproductive physiology in order to design a novel reproductive control tool.